

Table 2 – Comparison of corrugation with and without dampers 7 months after grinding

Wavelength	RMS roughness at low rail (μm)		
	Without damper	With dampers	% reduction*
80mm (250Hz)	6.32	1.76	72.2%
63mm (315Hz)	7.48	4.40	41.2%
50mm (400Hz)	3.44	3.09	10.2%
Overall 10-160mm (125-2000Hz)	10.86	6.03	44.5%

* Remark: % reduction is defined as (roughness w/o damper – roughness with damper)/roughness w/o damper x 100%

6 SUMMARY

Rail dampers were installed on a curved track of 300m radius to study the reduction of noise radiation and investigate the long term effect on corrugation growth. The saloon noise level was reduced by around 3dB(A). Overall vertical and lateral track vibration levels were reduced by 7dB(A) and 10dB(A) respectively.

Short-pitch corrugation of wavelengths of 50-80mm was observed at the low rail. Overall corrugation growth rate for critical wavelengths (10-160mm) was reduced by 45% after installation of rail dampers. The findings reveal that the corrugation growth at the test site is approximately linear and independent of original roughness.

ACKNOWLEDGEMENTS

The first author wishes to express sincere thanks to MTR Corporation for their provision of testing sites and approval for publishing of the paper content.

References

- [1]. Létourneau F. et al., *High Speed Railway Noise: Assessment of Mitigation Measures*, Notes on Numerical Fluid Mechanics and Multidisciplinary Design Vol.99, p56-62 (2007)
- [2]. Asmussen B. et al., *Reducing the Noise Emission by Increasing the Damping of the Rail: Results of a Field Test*, Notes on Numerical Fluid Mechanics and Multidisciplinary Design Vol.99, p229-235 (2007)
- [3]. Nelson T.: *TCRP Report 67 – Wheel and Rail Vibration Absorber Testing and Demonstration*, Transportation Research Board, Chapter 9, 42-44 (2001).
- [4]. Thompson D.J. et al., *A Tuned Damping Device for Reducing Noise from Railway Track*, Applied Acoustics 68 (2007), 43-57.
- [5]. W. Ho, B. Wong, D. England, *Tuned Mass Damper for Rail Noise Control*, Notes on Numerical Fluid Mechanics and Multidisciplinary Design Vol.118, p89-96 (2010)
- [6]. B.E. Croft, C.J.C. Jones, D.J. Thompson, *Modeling the effect of rail dampers on wheel-rail interaction forces and rail roughness growth rates*, Journal of Sound and Vibration vol.323, p17-32 (2009)
- [7]. T.X. Wu, *Effects on Short Pitch Rail Corrugation Growth of a Rail Vibration Absorber/Damper*, Wear Journal vol.271, p339-348 (2011)
- [8]. T.X. Wu, D.J. Thompson, *An Investigation into Rail Corrugation due to Micro-Slip under Multiple Wheel Rail Interactions*, ISVR Technical Memorandum No.887 (2002)
- [9]. W. Ho, B. Wong, D. England, A. Pang and C.W.S To, *Reduction of Corrugation Growth Rate by Rail Dampers*, to be published in TDHRail Magazine Nov 2012 Issue

浮置板減振對地鐵車內噪聲的影響

The effect of floating slab for vibration damping on noises in metro cars

毛東興、邵志跃

MAO Dong Xing, SHAO Zhi Yue

(中华人民共和国 上海市 四平路 同济大学声学研究所)

(Institute of Acoustics, Tongji University, Siping Road, Shanghai, PRC)

Abstract: As metro developing, quantities of noise and vibration pollution problems emerge. Researches showed track bed with floating slab laid would cause less vibration on the foundation than the traditional one. Although the effects of floating slab on vibration damping and noise reduction are significant, the influences on noise in metro cars are still unknown. So the tests of noise in metro cars which traveled on track with and without floating slab were taken. With statistical analysis, results revealed different noise characteristics in metro cars between the two train travelling conditions, and especially the noise at low frequencies under the former condition were obviously louder. Hence the floating slab may amplify the low frequencies noise in metro cars.

Key words: acoustics; floating slab; noise in metro cars

摘要：轨道交通日益发展，随之产生诸多噪声和振动的环境污染问题。研究表明，轨道中铺设浮置板道床相对于传统道床具有良好的减振效果。对周围环境的噪声和振动影响减小，而对列车内噪声的影响还不得而知。因此在铺设浮置板道床及普通道床的列车运行区间进行车内噪声测试，经多次测试得到具有统计意义的结果，表明列车在两种道床运行时车内噪声具有明显差别，前者车内低频噪声较高。所以，可认为浮置板对车内低频噪声起到“放大”作用。

关键词：声学；浮置板；地铁车内噪声

1 引言

近年来城市建设快速发展，轨道交通已成为大中城市极为重要的交通方式之一。一线城市地铁运营里程均达数百公里，并在持续发展；多个二线城市地铁运营里程也达数十公里，将不断有城市地铁新建运营；个别三线城市地铁也建设之中。可见，我国将形成庞大的城市轨道交通系统。由于轨道交通的便利、通达等特点，轨道交通线路一般都穿行于城市工作、生活密集区，因此，轨道交通噪声和振动辐射极易对周围环境产生影响。据统计，2008~2009年上海市轨道交通沿线居民集中投诉点60多个，除施工引起的房屋开裂外，受到振动和噪声困扰引发的投诉占40%以上，室内振动及二次结构噪声极大地干扰了居民的正常生活^[1]。因此，国内外研究者长期致力于对轨道交通的减振降噪措施的研究。对于轨道结构减振措施中，根据采取隔振措施的部位划分^[2]为钢轨类、扣件类、轨枕类和道床类，而道床类隔振一般以橡胶浮置板和钢弹簧浮置板道床为主。大量研究^[3-5]和实测^{[1][6][7]}表明，浮置板道床能够起到较好的减振作用，其中钢弹簧浮置板道床相对于橡胶浮置板道床又具有便于维护更换，及减振效果更加理想的特点。

然而，道床类减振措施虽然对于降低对外部环境的振动噪声影响具有明显效果，但是鲜有关注其对列车内部噪声与振动的影响，而这与列车内乘客的乘坐舒适体验息息相关。有文献^[8]指出列车通过铺设橡胶浮置板道床地段时，车内振动和噪声明显增大。而钢弹簧浮置板道床是否会有类似影响有待于研究，因此在安装钢弹簧浮置板道床的轨道区间，对列车运行时车内噪声进行了实测。

2 车内噪声测量

2.1 测量轨道条件

测量在南京地铁 1 号线中一段铺设钢弹簧浮置板道床区间进行，其中上行方向两站间近到达站站台 120m 线路段铺设了钢弹簧浮置板，其余为普通道床段；下行方向两站间近出发站站台 120m 线路段铺设浮置板，其余为普通道床段。

为了更好地进行安装钢弹簧浮置板道床前后对车内噪声影响的对比分析，试验还在上行方向到达站至下一站及下行方向出发站上一站至出发站间分别进行了测量，这两段区间道床均为普通道床。

2.2 测点布置及测量仪器

上行方向均在列车车厢前端进行测量，下行方向在列车车厢末端进行测量。测点距车厢地面高度为 1.5m。

噪声测试仪器采用的是 National Instruments 公司的 NI 9234 多通道采集系统。测量传声器为声望 (BSWA) 的 MPA201 型传感器。

2.3 列车运行条件/测量次数

试验过程中，视频记录列车速度仪表盘，与所记录音频文件相对应，以得到列车通过浮置板道床区段的运行速度。上行方向列车在通过浮置板道床段时即将或已开始减速，下行方向列车在通过浮置板道床段时处于加速阶段。

测量在上行和下行方向各重复多次进行。测量过程中一些测量数据会受到外界环境的干扰，因此，实际测量的列车运行次数根据测量数据的情况及时调整，以使测量结果具有较好的一致性和稳定性。

测量时间选取在夜间 22:00 以后至运营结束，以及早晨 5:30~9:00 之间客流较少的时间段，以减少车厢内人员对测量的干扰。

2.4 数据处理和评价量

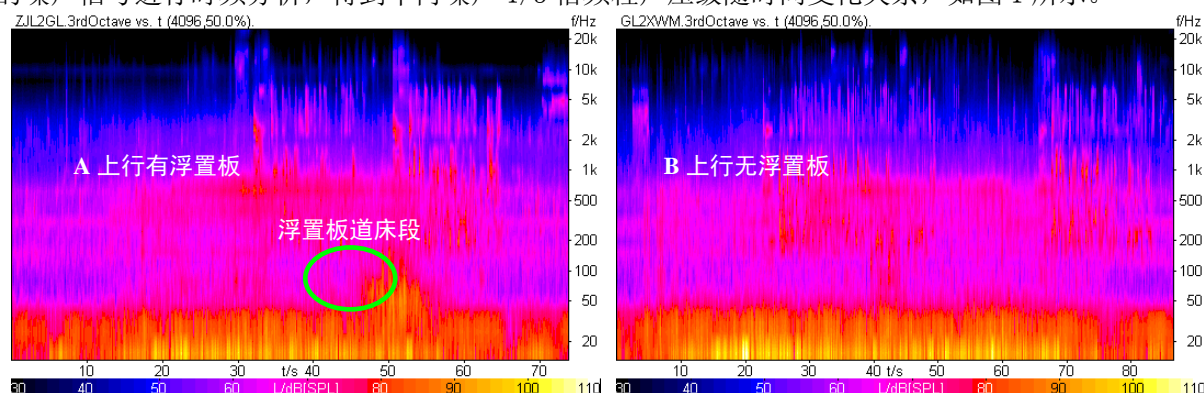
测量过程中完整记录列车于两站之间运行的时间历程。根据记录的时间历程，截取记录数据中列车通过浮置板道床段的信号以及对应的普通道床段的信号作为测量的分析数据，将各种条件下多次测量结果分别取平均值。列车通过浮置板道床段的信号分为有/无语音干扰两部分，对比语音信号对数据结果的干扰程度。

测量分析量中给出列车通过浮置板及对应普通段道床时的 1/3 倍频程频谱声压级以及线性、A 计权声级，两种情况 1/3 倍频程频谱声压级以及线性、A 计权声级的差值。

3 测试结果及分析

3.1 经过有/无浮置板道床车内噪声对比

利用 Artemis 软件，将上下行列车在铺设浮置板道床的两站区间及无浮置板道床的两站区间运行时记录的噪声信号进行时频分析，得到车内噪声 1/3 倍频程声压级随时间变化关系，如图 1 所示。



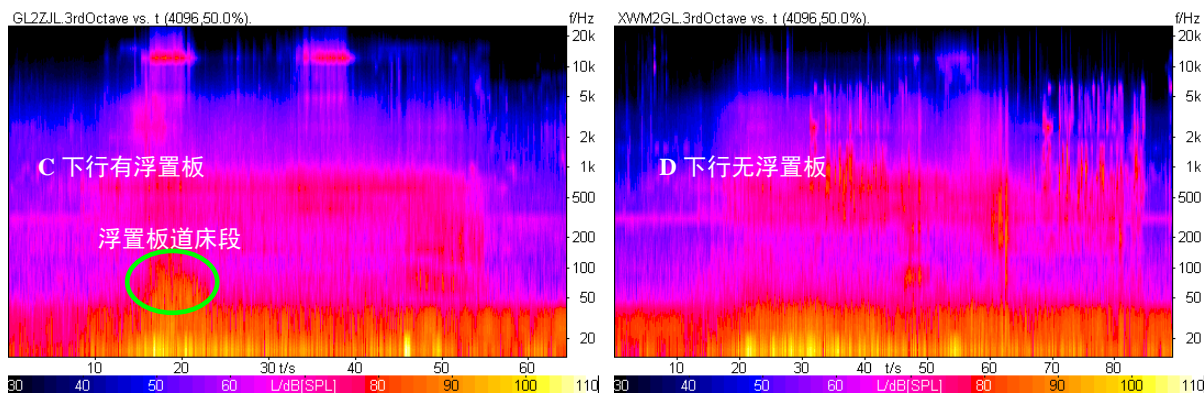


图 1 上下行方向列车通过有/无浮置板道床两车站间列车车内 1/3 倍频程声压级随时间变化(A, 上行有浮置板; B, 上行无浮置板; C, 下行有浮置板; D, 下行无浮置板)

不难发现，列车在通过浮置板道床段，车内噪声频谱出现明显变化，低频噪声显著增加，其他频段没有显著异常。对应列车通过此区间时在车厢内的乘坐体验，乘客明显听到低沉的轰隆声，影响乘坐舒适性。

为了详细研究列车通过浮置板道床段车内噪声特征，将所记录两站之间完整时间历程中经过浮置板道床段的信号截取。利用软件进行频谱分析，得到列车通过浮置板及对应普通段道床时的 1/3 倍频程频谱声压级以及线性、A 计权声级，以及两种情况 1/3 倍频程频谱声压级以及线性、A 计权声级的差值，如图 2 所示。

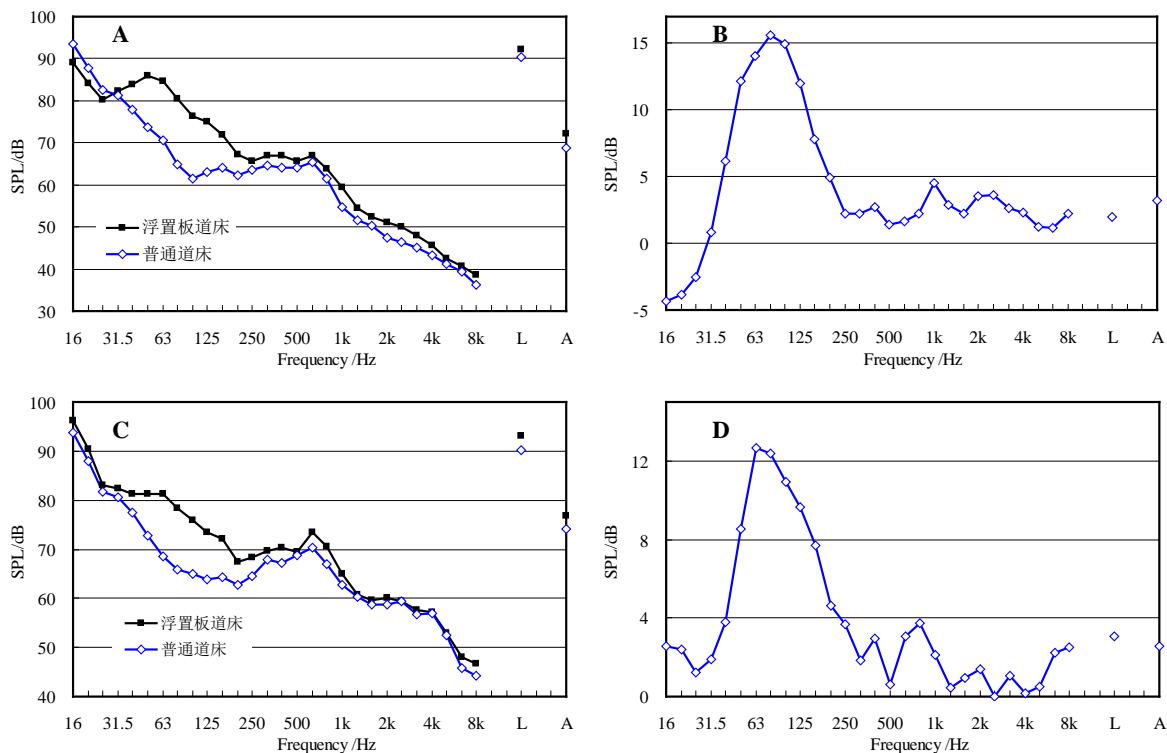


图 2 上下行方向列车通过有/无浮置板道床区间列车车内噪声 1/3 倍频程频谱、线性和 A 声级和两种情况的差值
(A, 上行有/无浮置板道床; B, 上行两种情况差值; C, 下行有/无浮置板道床; D, 下行两种情况差值)

从图 2(A)可以看出，上行方向列车通过浮置板道床段及普通道床的频谱差异主要集中在 40~200Hz，所引起的低频噪声要显著高于普通道床段。图 2(B)显示以 80Hz 为中心的前后两个倍频程范围，列车通过浮置板道床区间比普通道床的声压级高 5dB 以上，在 80Hz 高出 15.6dB；由于 16Hz 处声压级对总体线性声压级贡献较大，导致两者线性声压级相差不大；A 计权声级增加 3.2dB。

从图 2(C)中可以看出，下行方向列车通过浮置板道床区间所引起的低频噪声增加依旧集中在 40~200Hz 范围。图 2(D)显示与上行方向类似曲线，峰值出现在 63Hz 为 12.7dB。线性声压级与 A 计权声级的增加量与上行类似，分别为 3.1dB 和 2.5dB。

3.2 语音干扰及运行方向对测试结果的影响

将包含语音干扰和未被干扰的上行列车通过浮置板道床区间的信号进行频谱分析，及上下行列车通过浮置板道床区间的信号进行频谱分析，如图 3 所示。

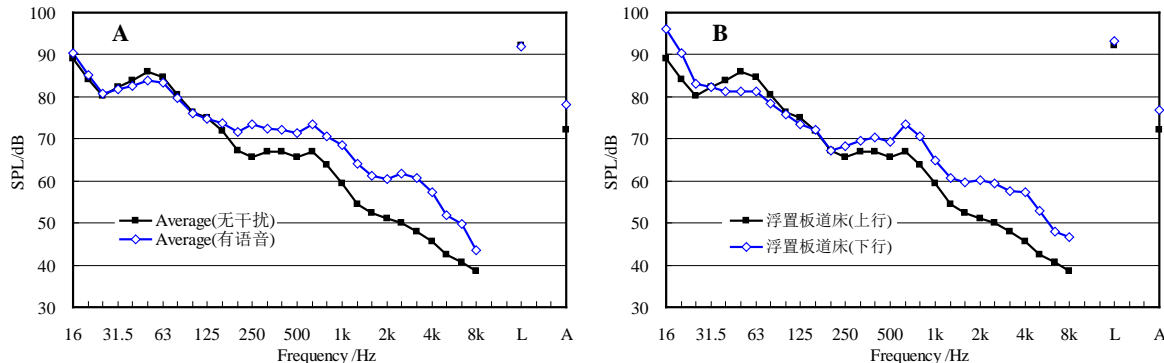


图 3 上行方向列车通过浮置板道床区间有/无语音干扰时列车车内噪声 1/3 倍频程频谱、线性及 A 声级及上下行列车通过浮置板道床区间车内噪声 1/3 倍频程频谱、线性及 A 声级 (A, 上行有/无语音干扰; B, 上下行噪声频谱对比)

由图 3(A)知，语音干扰主要影响 250Hz 以上的中高频声压级，对浮置板所影响的 250Hz 以下的低频范围几乎没有干扰。由图 3(B)知，上行方向列车通过浮置板道床激发的噪声在 63Hz 附近范围内高于下行方向。列车在上行方向通过浮置板道床段时，处于即将或刚开始减速运行工况；而下行方向，处于启动后加速运行工况，差异主要由车辆动荷载以及车速的不同引起。中高频的差异主要由测试中语音干扰以及各自轮轨相互作用的不同等因素引起，与浮置板道床引起的噪声变化无关。

4 总结

结合上述数据及分析，总结得到以下结论：1. 浮置板道床段的车内 A 计权声级增加量 3dB(A)左右。2. 实际测试中语音干扰集中在中高频范围，并未对浮置板道床引起的车内噪声频谱变化造成影响，用低频噪声声压级变化来评价更能表现出浮置板道床对车内噪声的影响。3. 在所测实际情况中，列车在减速运行条件下，车内 63Hz 附近的低频噪声高于加速条件下的车内噪声级。

考虑到钢弹簧浮置板起到较好减振作用的频率范围与车内低频噪声显著增加的频率范围相似，列车内低频噪声增加的原因，有待于进一步结合道床、轨道和列车间的相互作用进行深入探讨。

References

- [1] 夏丹, 周裕德, 祝文英, 张玮晨, 应乐淳, 储益萍. 上海地铁减振措施及效果测试分析 [J]. 噪声与振动控制, 2009, **29**(S2): 214-217.
- [2] 孙洪强. 简析城市轨道交通减振降噪措施 [J]. 现代城市轨道交通, 2012, (4):60-63.
- [3] Cui F, Chew C H. The effectiveness of floating slab track system — Part I. Receptance methods [J]. Applied Acoustics, 2000, **61** (4): 441-453.
- [4] Hussein M F M, Hunt H E M. Modelling of floating-slab tracks with continuous slabs under oscillating moving loads [J]. Journal of Sound and Vibration, 2006, **297** (1-2): 37-54.
- [5] Hui C K, Ng C F. The effects of floating slab bending resonances on the vibration isolation of rail viaduct [J]. Applied Acoustics, 2009, **70** (6): 830-844.
- [6] 孙成龙, 高亮. 北京地铁 5 号线钢弹簧浮置板轨道减振效果测试与分析 [J]. 铁道建筑, 2011, (4):110-113
- [7] 张宝才, 徐祯祥. 螺旋钢弹簧浮置板隔振技术在城市轨道交通减振降噪上的应用 [J]. 中国铁道科学, 2002, **23** (3): 68-71.
- [8] 高世兵. 钢弹簧浮置板减振轨道在城市地铁中的应用 [J]. 铁道工程学报, 2008, **114**(3):88-91.

鐵路站的公共廣播系統設計 Public Address System Design in Railway Stations

何偉麟、吳子聰、王錦新

Wilson HO, Eddy NG, Banting WONG

(威信聲學顧問有限公司，香港特別行政區沙田源順圍沙田工業中心 A 座 601 室)

(Wilson Acoustics Limited, Unit 601, Block A, Shatin Industrial Centre, Yuen Shun Circuit, Shatin, Hong Kong SAR)

Abstract: Railway station Public Address (PA) system plays a crucial role in the communication between station control and passengers. Nowadays, most railway station PA systems are designed to provide Voice Alarm (VA) function in addition to routine operation announcements. VA system aims to alert people to an emergency in a clear and unambiguous manner with minimum delay. Therefore, it has to provide uniform and intelligible messages to all passengers in the emergency excavation zone even in a great crowd of rushing people. Many early designed railway stations possess architectural features promoting adverse reverberance. A proper PA loudspeaker system design becomes a feasible solution to overcome the detrimental acoustic environment inherent by the station architectural design, and improve the broadcasting quality to achieve PA and VA functions. According to the experience obtained from the PA design and commissioning on MTR LAR, WIL, SIL, KTE, XRL and TAP (total 22 stations), the authors review the PA design common practice and the applicability of speech intelligibility theories in various architectural acoustic conditions. With this knowledge, specialist contractors, consultants and end users should be able to assess their acoustic needs and install the proper loudspeaker systems for PA and VA functions.

Key words: Public Address System; Speech Intelligibility; Railway Station; Design

摘要：公共廣播系統在鐵路通訊系統是不可缺少的一部分。現今主要鐵路站的公共廣播系統除了作日常資訊廣播外亦配備語音警報功能。語音警報能於意外發生時迅速作出清晰的提示，讓站內人員能夠疏散至安全區域。許多早期設計的鐵路站因缺乏建築聲學考慮導致站內存在大量餘響，精確的廣播系統設計能提升訊息廣播質量，從而有效地發揮其廣播和語音警報功能。根據作者在香港各段鐵路線的廣播系統設計及測試之經驗（包括東涌及機場快綫、西港島綫、南港島綫、官塘延線、西九高鐵總站及大埔東站），本文概述廣播系統設計的普遍法則和語音清晰度的基礎理論。這些知識使系統安裝承辦商、聲學顧問及使用者能更有效地評估不同的聲學需求和安裝合適的公共廣播系統。

关键词：公共廣播系統；語音清晰度；鐵路站；設計

1 INTRODUCTION

The PA system is commonly found in railway stations, which act as a commination system in which pre-recorded or live messages are conveyed to passengers for routine operation announcements and emergency broadcast for giving instructions to direct them to emergency excavation zones. For a PA system to be effective in transportation amenities, the deliverable must be clear, uniform and intelligible. Generally, in order to achieve sufficiently high degree of speech intelligibility, increasing the direct-to-reverberant ratio by adding acoustic absorption in the architectural surface finishes is a common practice. However, this approach is quite costly and sometimes impractical for space where architectural alteration is technically difficult. In this situation, proper PA system design is of particular essential for achieving good speech intelligibility in areas with challenging

acoustics^[1]. To achieve high speech intelligibility in railway stations, it can be stated that the radiation characteristic is one of the most important features of a PA system. The rule of thumb of PA system design is simply to direct the sound to where it is needed and avoid radiation onto unoccupied areas causing reflections. Furthermore, the sound pressure level (SPL) at the listener positions has to be high enough to ensure a sufficient signal-to-noise (S/N) ratio. This paper describes some basic knowledge about room acoustics, the requirement for speech intelligibility in railway station and shows the common practice on laying out the PA loudspeaker system.

2 PA SYSTEM PERFORMANCE REQUIREMENTS

Speech Intelligibility is the degree to which human listeners comprehensible to the voice messages. It is becoming an increasing concern in PA systems. Several quantitative based speech intelligibility assessment methods have been used nowadays. Perhaps most recognized one is the calculation of speech transmission index (STI) based on IEC 60268-16 “Sound system equipment - Part 16: Objective rating of speech intelligibility by speech transmission index”^[2]. This method rates intelligibility on characterization of reduction in original speech modulation at a receiver position and give a non-linear scale from 0 to 1, 0 indicates completely unintelligible while 1 represents perfectly intelligible. Table 1 summarizes the STI values and the corresponding ratings. According to BS7443^[3] and BS5839 Part8^[4] which declared that any public area of a railway stations have to achieve a minimum of 0.5 RaSTI values, based on a minimum S/N ratio of 15dB. The RaSTI index is the simplification of STI, which is sufficient for characterizing speech intelligibility for PA systems. At a RaSTI of 0.5, 97% of sentences known to listeners would be correctly understood, while 94% of sentences presented to listeners for the first time would be correctly understood as shown in Table 2. In general practice, uniform SPL distribution should also be achieved within each active zone such that the variation of SPL shall be maintained within a range of ± 3 dB of the mean level with the ambient noise sensing devices disable.

Table 1 – Sound transmission index (STI) scale and corresponding ratings

STI	Rating
0.75-1.0	Excellent
0.60-0.75	Good
0.45-0.60	Fair
0.30-0.45	Poor
0.00-0.30	Bad

Table 2 – Relationship between STI and speech intelligibility

Test	Percentage understood correctly		Subjective rating scale	
	RaSTI = 0.50	RaSTI = 0.60	RaSTI = 0.50	RaSTI = 0.60
Sentences (known to listeners)	97%	98%	Good	Very Good
Sentences (1 st presentation to listeners)	95%	98%	Fair to Good	Good to Very Good
PB words*	74%	87%	Fair	Good
Nonsense Syllables	69%	84%	Fair	Good

*Phonetically balanced words consisting of a consonant, vowel, and consonant, which are typically difficult to distinguish from other words.

3 FACTORS AFFECTING PA SYSTEM PERFORMANCE

Speech is not just necessarily to be audible. Having enough speech level is a must, but not enough for good speech intelligibility. A loud, but reverberant speech signal can be completely unintelligible. The performance of a PA system relating to its intelligibility is quite complicated and depends on multiple factors. Some of these factors are related to the acoustic environment of the space and others are inherent within the electronics of the system. In general, speech intelligibility is mostly affected by both background noise level and the acoustic of the space concerned. Below illustrates the major parameters that affect speech intelligibility along the source to listener transmission path.

3.1 Reverberation and echo

Reverberation and echo from acoustically hard surfaces are the primary causes for low speech intelligibility in railway stations. In general, if echoes arrive 80ms later than the first arrival sound, they can harm speech intelligibility^[5]. In continuous speech, the echo from a previously uttered syllable masks or obscures the sound of subsequent syllables, making speech more difficult to understand. Reverberation is made of multiple sound reflections that have the effect of smearing, or blurring speech, making it less clear and non-distinguishable. It is widely accepted that a reverberation time of 1.5s at mid-frequency is the maximum time that allow for achieving intelligible speech.

3.2 Background noise

The noise levels at different locations are different ranging from quiet to noisy in a railway station. Noise from passenger conversation, train running and mechanical equipment has the effect of masking the announcements and cause serious reduction in speech intelligibility. It is understood that ideally a S/N ratio of 15dB above is conductive to good speech intelligibility.

3.3 Sound system distortion

The distortion of electrical or electro-acoustical components in the PA system can result in the generation of noise that masks the original speech signal. Severe amplifier clipping, for example, can make a perfect speech signal at the input to the amplifier more difficult to understand at the output.

4 BASIC PA SYSTEM DESIGN PRINCIPLES

Generally, sound-absorbing treatment would be incorporated in the architectural design of a railway station to control excessive reverberant sound. However, in some early designed railway stations, acoustical problems of uncomfortable and difficulties in hearing public address announcement are often occurred due to poor acoustical treatment such as hard and reflective floors, tall and non-sound absorptive ceilings which comes along with long reverberation time. The aesthetics of the station usually not allowed to be materially altered. For this kind of spaces, a proper PA system loudspeaker selection and layout is of particular essential for achieving sufficient speech intelligibility in areas with challenging acoustics.

4.1 Loudspeaker type and properties

It is essential for a successful PA system design that the correct type of loudspeaker is chosen. PA system loudspeakers used in typical railway stations usually consists of 4 major types, namely ceiling loudspeaker, wall-mounted loudspeaker, column loudspeaker and horn loudspeaker. The type of loudspeaker to be used depends on many factors including the room dimension, architectural structure features of the application space concerned as well as the loudspeaker properties. There are two main parameters that are commonly used to preliminary characterize loudspeaker properties, i.e. sensitivity and directivity. The sensitivity of a loudspeaker is the SPL expressed in decibel (dB) at 1kHz and at a distance, on axis, of 1m with an input power of 1W. The greater the sensitivity, the higher will be the output SPL at a given position. The directivity of a loudspeaker is usually defined in an opening angle and describe in a form of frequency dependent polar diagram, which is the dispersion of a sound that radiates from the front of the loudspeaker. The opening angles are the angles at which the output from the loudspeaker is 6dB less than that produced on the main axis of the loudspeaker. Dependent upon the environment and the particular application needs, it may be necessary to use loudspeakers with a wide opening angle, which spread their sound over a wide area. Alternatively it may be necessary to concentrate a beam of sound in a particular direction. Table 3 summarizes the sensitivity and directivity of the typically used loudspeakers and their corresponding application areas.

Table 3 – Comparison of different typically used PA system loudspeakers

Loudspeaker Type	Loudspeaker Features and Application Area	Sensitivity	Opening Angle (Horizontal)
Ceiling	<ul style="list-style-type: none"> ▪ Easily recess into ceiling void or hollow wall. ▪ Used in areas of ceiling height up to 6m. ▪ Easily spaced at a regular intervals to give fairly uniform sound coverage. ▪ Difficult to achieve good intelligibility for RT > 2.0s. 	88dB(A) – 95dB(A)	150° - 210° (at 1kHz)

Wall-mounted	<ul style="list-style-type: none"> Convenient for mounting on walls or pillars. Greater throw distance than ceiling loudspeaker. Suitable for floor to ceiling height less than 4m. 	90dB(A) - 96dB(A)	120° - 180° (at 1kHz)
Column	<ul style="list-style-type: none"> Broad horizontal sound coverage similar to ceiling speaker. Directional and narrow vertical sound beam (10°-15°). Desirable in reverberant environment where sound direct to listener only without reflecting off hard wall and ceiling. 	88dB(A) - 96dB(A)	180° - 220° (at 1kHz)
Horn	<ul style="list-style-type: none"> High sensitivity and high sound pressure level. Narrow and directional coverage pattern. Produce a powerful, concentrated, beam of sound enabling them to reach listeners at a great distance. Usually high frequency response is limited. 	96dB(A) - 130dB(A)	70° - 160° (at 1kHz)

4.2 Loudspeaker arrangement and setting

In order to provide maximum flexibility in directing announcements to individual areas, railway station should normally be divided into different PA zones. Each zone would have its own amplifier, ambient noise sensing, an automatic level control, and spectrum equalization. After selection of appropriate type of loudspeakers, the sensitivity and opening angle should be used initially to predict the coverage and plan an installation. When laying out and positioning loudspeakers, primary consideration should be given to the difference in SPL between the position on the main axis of the loudspeaker and at the same distance at an off-axis position. A 6dB difference would be quite noticeable and is sufficient to affect speech intelligibility in a noisy and reverberant environment. It is essential that the announcement sound level is loud enough at noisy locations, but not too loud at quiet locations.

In a traditional layout approach to overhead-distributed ceiling loudspeakers, loudspeakers are located in a grid arrangement whose positions are dictated by the ceiling height, the sensitivity and the directivity of loudspeakers. Two basic placement patterns prevail: square spacing and hexagonal spacing. A square pattern lines up the row and column of speakers in a square pattern. On the contrary, row of speakers are offset from each other in hexagonal pattern (Figure 1a). The choice of a square or hexagonal layout is usually a function of room dimensions and shape. Square spacing pattern gives higher evenness of sound coverage with fewer loudspeakers in general. In addition to the placement pattern, loudspeaker density is also an important factor that affects sound uniformity and speech intelligibility. Generally, three density patterns are usually applied namely edge-to-edge, minimum overlap and full overlap (Figure 1b). The greater the overlap, the more uniform the sound coverage and higher SPL level would be. Equation 1 shows the calculation method for determining maximum spacing between ceiling loudspeakers that variation of SPL less than 6dB could be obtained.

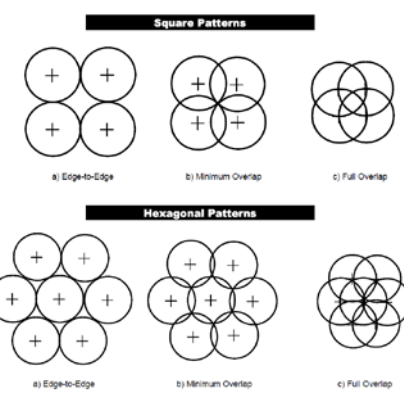
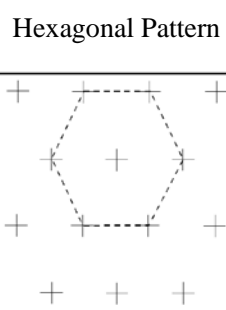
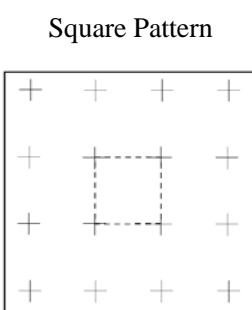


Figure 1 – (a) Ceiling loudspeaker placement pattern

(b) Ceiling loudspeaker density pattern

A common used calculation method leads to the maximum spacing between ceiling loudspeakers:

$$D = 2 H \tan (\alpha/2) \quad (1)$$

where:

$H = (h-l)$ = Ceiling height to Ear height

α = opening angle at particular frequency concerned

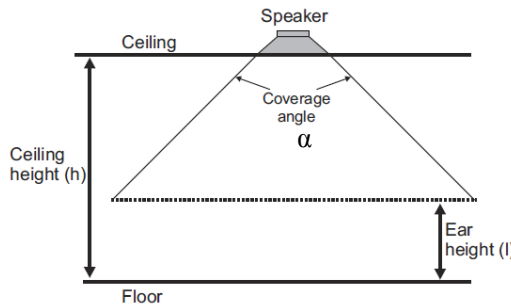


Figure 2 – Ceiling loudspeaker coverage

For column loudspeaker distribution system, the loudspeaker spacing should be less than 15m apart when facing in the same direction in order to avoid signal delay arising from neighbor loudspeakers. Since the throw distance of wall-mounted projector is limited, the loudspeaker spacing should not be greater than 6m for uniform sound coverage. The loudspeaker should be angled downwards to cover the appropriate area and to limit the overspill to adjacent areas. The typical mounting height for wall-mounted projectors and column loudspeaker are around 2.5-4m. Figure 3 illustrates the typical loudspeaker distribution pattern for wall-mounted or column loudspeakers.

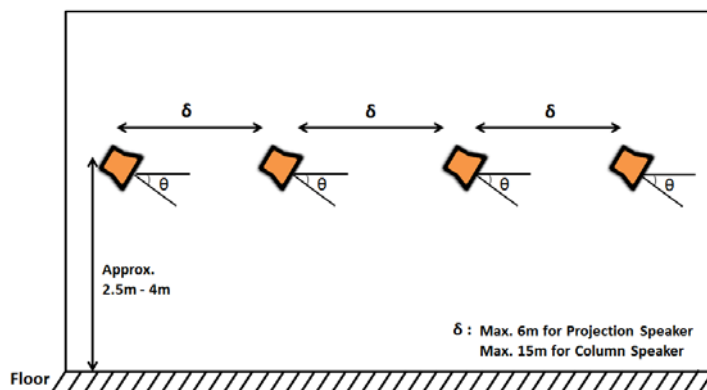


Figure 3 – Typical wall-mounted or column loudspeaker distribution pattern

After the distribution pattern of loudspeakers is selected, it is necessary to calculate the SPL at the positions where sound coverage is required. To disseminate messages with good speech intelligibility, the level at any area should be 15 dB above the ambient noise. The sensitivity may be used to calculate the SPL at any distances away from the loudspeaker center. The inverse square law defines the relationship between input power and SPL as well as between distance and SPL, which states that each time the input power of a loudspeaker is doubled, the SPL rises by 3 dB, while the SPL drops by 6 dB each time the distance is doubled. Mathematically, these relationships are described as below.

$$SPL_A = SPL_{1.1} + 10 \log P/P_0 - 20 \log r/r_0 \quad (2)$$

where:

SPL_A = SPL for input power at measured distance $SPL_{1.1}$ = sensitivity of loudspeaker in dB for 1W/m

P = input power (W) P_0 = reference power (1W)

r = measured distance (m) r_0 = reference distance (1m)

To achieve reasonable speech intelligibility in a harsh acoustic environment, it is usually preferable to use a large number of uniformly spaced loudspeakers at relatively low tap settings, instead of a small number of speakers at high levels. This increases the direct sound energy reaching the listener's ears and reduces the harmful reverberant energy. Best results are obtained when the ceiling loudspeakers are mounted with their axes vertical and are spaced close enough together so that the coverage patterns overlap.

4.3 Automatic volume control

In a railway station, the ambient noise is rather time-independent, non-uniform and significantly affected by other noise sources. Consider a train station platform as an example, the noise level is particular low without train services, however, the noise level increase significant when the train approaches and decreases as the train stops. The announcement can be quite easily heard when train has not yet arrived, but the message becomes less comprehensible while the train is arriving. Therefore, the temporal PA system performance can differ significantly. The fluctuated ambient noise level could be overcome using automatic volume control in each PA zone, so as to maintain a consistent S/N ratio for announcement broadcast.

5 SUMMARY

In a railway station, sufficient speech intelligibility is required for passengers to comprehend announcements from the PA system. Understanding speech intelligibility and its associated influencing factors is of particular importance for proper design of PA systems. This paper reviews the basic of speech intelligibility and PA system design principle. With this knowledge, PA system designer would be able to assess their acoustic needs and install the proper loudspeaker systems for PA and VA functions.

References

- [1] Wilson Ho, Eddy Ng: *Public Address System Reinstallation*, Acoustic 2012, Hong Kong
- [2] IEC 60268-16 (2003-05), “*Sound System Equipment – Part 16: Objective Rating of Speech Intelligibility by Speech Transmission Index.*”
- [3] BS 7443: 1991. *Sound Systems for Emergency Purposes*, 1991 (British Standards Institute, London).
- [4] BS 5839-8:2008 – “*Fire detection and alarm systems for buildings. Code of practice for system design, installation, commissioning and maintenance of voice alarm systems.*”
- [5] J. S. Bradley, H. Sato, M. Pickard: *On the importance of early reflections for speech in rooms.* J. Acoust. Soc. Am. 113(6) (2003) 3233-3244.H.

室內語音清晰度與聲源寬廣度對大腦皮質上腦波之影響研究

The Influence for Cortical brainwaves in relation to word Intelligibility and ASW in Room

陳炯堯

CHEN Chiung Yao

(中華民國 台中霧峰朝陽科技大學 建築系)

(Architecture Department, Chaoyang University of Technology, 168, Gifeng E. Rd., Wufeng, Taichung, ROC)

Abstract: To study the effects of word intelligibility and apparent sound width (ASW) by changing the initial delay gap between direct and first reflection, (Δt_1) and inter-aural cross-correlation function (ICF) in room, the features of the reactions on cortical continuous brainwave's ACF and auditory evoked potential (AEP) were analyzed. The qualities of brainwave's ACF and AEP were obtained by the stimuli of mono-syllables and pure tone pulse (2 kHz). The results show: 1. The effective duration of ACF (τ_e) of β -waves (13 ~ 30 Hz) on left hemisphere correlated well ($p<0.001$) with word-intelligibility; 2. The volt level differences (VLD) of slow vertex responses (SVR) on A(P2-N2) decreased with the ASW ($p<0.05$), and the latencies at N2 (reference to P1 position) prolonged with ASW on lateral lemniscus of auditory path; 3. Due to hemispheric specialization in brain, the temporal effect of word intelligibility dominates over left hemispheres, but the effect of ASW incoherently responds by spatial consciousness on right.

Key words: brainwaves; ACF; word difficulty; apparent sound width; subjective diffuseness; hemispheric specialization

摘要：以聲場初期反射能量遲延時間(Δt_1)與空間雙耳互函數兩因子作為變因，來研究室內語音清晰度與聲源寬廣度對大腦皮質上腦波反應的影響。刺激音訊分別為單音節語音與純音(2 kHz)脈衝；並分別以連續腦波自函數與聽性喚起電位之波形變化進行比較。結果顯示：1. Δt_1 改變下左腦的 β 波(13 ~ 30 Hz)自函數的有效遲延時間(τ_e)與空間語音的清晰度得到顯著正相關($p<0.001$)；2. 空間聲源寬廣度增加時，左腦波形振幅差 A(P2-N2)在慢性頭頂反應(SVR)中呈現減少趨勢($p<0.05$)；且 N2 之潛時相對於波峰 P1 也出現增長($p<0.05$)的趨勢，反應部位推測是聽覺神經路中的外側蹄系；3. 在左右腦對聲場時間與空間專門化議題上，時間因素為主的語音清晰度很明顯是由左腦所控制。而空間主觀聲源寬廣度對腦波的影響卻也在左腦；證明受測者專注在主觀擴散時腦波並未必反應在右腦。

关键词： 腦波；自函數；語音清晰度；聲源寬廣度；主觀擴散；大腦專門化

1 研究源起

語音清晰度在人類語言認知中屬於短期記憶(short-term memory)與大腦回饋作用的綜合體(Schmidt & Wrissberg, 2000)。然而，對於聲音空間印象的評價指標中，聆聽者對聲源方向的判斷(方向感)、距聲源遠近的判斷(親切感)、聲源寬廣度(apparent source width, ASW)及聲音包被感(lateral envelopment, LEV)等，都是組成空間印象的重要元素。Ando (1985) 認為這種空間印象的構成主要是決定於空間雙耳互函數級數(the magnitude of the interaural cross-correlation, IACC)的變動，特別是對於聲場的主觀擴散程度有一定的影響程度。然而主觀擴散與聲源寬廣度對聽者而言卻表現出不同的需求與感受型態。在神經心理學(neuron-psychology)上，Sperry (1961)發現有大腦半球專門化(hemispheric disconnect)的現象，或以「言語機能」與「非言語

機能」的專職理論(cerebral specialization theory)來區分。在建築設計中，也有屬於非言語機能的象徵。如美感、均衡感知同屬於「非言語機能」的範疇。尤其在環境設計的領域裡，有不少是屬於非言語機能的象徵。然而，早期聲學與大腦關連性是以醫學上普遍之失語症或音律判斷障礙均發生於左大腦的受傷為起因。因此，我們假設瞭解物理環境中有關言語機能與非言語機能的大腦反應，將是替代有年齡層及文化差異問題之語意差(semantic difference, SD)實驗的最佳手段。因為音訊刺激與大腦生理反應特徵是跨越文化與年齡的一種最直接的研究參考指標。這與警方以生理反應來進行測謊是相同的道理。本研究假設在聲場設計上透過大腦反應來探討物理環境中的「言語機能」或語音清晰度變化時的反應應該是明顯且一致的。Ando (1983) 提到「言語機能」屬於時間要素(temporal factor)，是訊號自函數在腦部計算的結果；因此我們以語音清晰度影響下人的「主觀感受」與腦部反應之間的關連性來證明時間要素對環境之影響，以建立客觀之音環境設計基礎。Akita 等(1998)指出受測者所得到之感官情報以腦波來分析並非讓他們直接面對環境的改變，而是藉生理與環境之互動而來，它是日常生活中時時刻刻都存在的現象。其中大腦誘發強度是最理想的工具。Soeta 等(2002)在探討音源特性影響主觀心理與腦磁波 (MEG) 的反映是否相符研究中提到，當反射聲遲延時間改變 ($\Delta t = 0, 5, 20, 60$ 和 100ms) 並交替呈現 50 次記錄 MEG 中 α 波的自函數 (ACF) 有效遲延時間，可明顯反映出聲場的主觀喜好程度。

本研究方法歸納為下列二點：

1. 以改變聲場第一反射遲延(Δt)來改變語音清晰度，以中文語音單音節之主觀辨識度(或辨識過程)來與同期的大腦皮質上連續腦波(cerebral continuous brainwaves, CBW)的 α 與 β 波之自函數計算結果比較。
2. 以改變聲場雙耳互函數(IACC)來改變主觀聲源寬廣度，在受測者於感受空間聲源寬廣度時，與同期的大腦皮質上聽性喚起電位(AEP)的波形特徵變化量進行比較分析。

2 實驗方法

2-1 主觀心理實驗

本研究針對語音清晰度與聲源寬廣度的兩種主觀心理體驗透過單音節語音測聽與 IACC 調整兩種方式來進行量化改變。在語音清晰度部份，使用台灣地區常用中文單音節語音（陳炯堯等，2001）之音表第五組（女聲， 表 2-1），這組單音節語表為研究中檢測結果錯聽率落差最大，原因為此語表為「空韻」（係指舌尖元音「市」，如注音符號ㄓ、ㄔ、ㄕ、ㄕ、ㄔ、ㄕ為韻母之單音節）較多的檢測音表，空韻數量為八組與非空韻十組，數量較為平均。發音長度各約 $400 \sim 500\text{ ms}$ 進行實驗編輯。提示時，每一個字音間相隔 2.5 秒。實驗配置根據陳炯堯(1997)研究中之提示方式。實驗場地在朝陽科技大學半無響室中以面對受測者正前方，距離頭部中心 1.5m 位置的揚聲器 (Fostex NF-1A) 來提示直達音，而由另一個在縱向上方緊臨的揚聲器來提示第一反射音。並調整一般說話音量平均約 62 dB(A) 。實驗之物理參數設定如表 2-2。

表 2-1 單音節語音語表 (陳炯堯等, 2001)

音表一第五組			
1	ㄩˇ	10	ㄩㄞ
2	(ㄩ)ㄦ	11	ㄞㄨㄣ
3	ㄞㄧˇ	12	ㄞㄨㄤ
4	ㄞㄟˇ	13	ㄞㄧㄥˇ
5	ㄞㄞˇ	14	ㄞㄨㄥ
6	ㄞㄨˇ	15	ㄞㄚˇ
7	ㄞˊ	16	ㄞㄨㄛˋ
8	ㄞㄧㄠˇ	17	ㄏㄢˋ
9	ㄞㄡˇ	18	ㄞㄧㄝˇ

表 2-2 單音節語音主觀心理實驗之物理參數設定

項目	實驗條件設定
第一反射遲延時間	0 ms、35 ms、100 ms、150 ms、200 ms
揚聲器個別聲壓級	Direct Sound : 60 dB(A) $\Delta t: 55\text{ dB(A)}$

另外，在主觀聲源寬廣度的心理量化實驗部份是採用配對比較判別法 (paired-comparison method) 求得，實驗地點如前，距離受測者頭部中心 1.5m 位置的揚聲器（一個直達聲、二個反射聲）共三顆，以 2kHz 短純音 (1ms) 訊號為聲源，利用三顆揚聲器不同的入射角度與聲壓級來改變其聲場之 IACC (0.35, 0.57, 0.68, 0.81, 共四組)；藉此構成不同的主觀聲源寬廣度(表 2-3)。受測者（學生、共 80 位）以配對比較法分析判別聲源寬廣度的大小。實驗之聲音訊號樣本提示時間每一組中兩個樣本間之時間間隔為 2s，每組之間距為 10s，共有 6 組。受測者須做立即聆判(何者之聲源寬廣度較大)及記錄聽判結果，每份問卷之進行時間約為 1min。

表 2-3 2kHz 短純音構成不同聲源寬廣度的主觀心理實驗之物理參數設定值

IACC (setup values)	振 幅 A0	I1 聲壓位 準 dB(A)	振 幅 A1	I2 聲壓位 準 dB(A)	振 幅 A2	I3 聲級 dB(A)	ΣL 總聲 壓位準 dB(A)
0.35	1	62.6	0.8	59.4	0.8	59.4	65
0.57	1	62.6	0.8	59.4	0.8	59.4	65
0.68	1	55.4	0.4	53.4	0.4	55.4	65
0.81	1	64.0	0.2	53.4	0.2	53.4	65

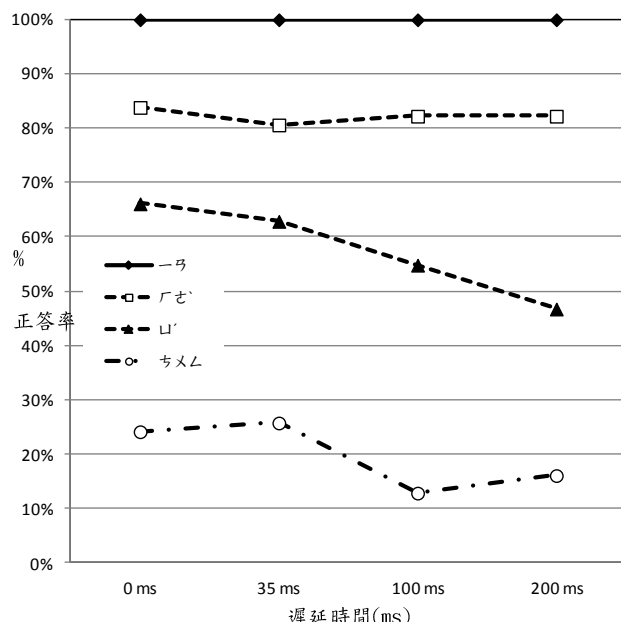


圖 2-1 單音節語音正答率與遲延時間之關係圖

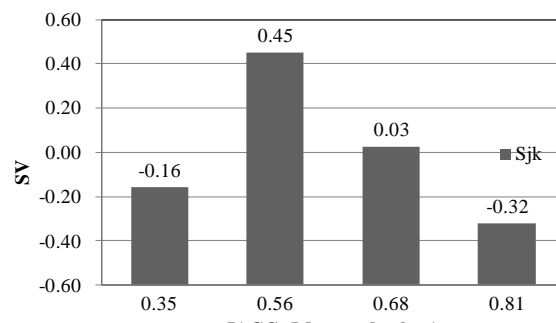


圖 2-2 主觀聲源寬廣度的心理量化值與 IACC 之關係圖

2-2 腦波生理實驗的方法

腦波經由快速傅立葉轉換(FFT)後，分別依左、右腦之 α 波(8–13 Hz)與 β 波(13–30 Hz)進行腦波之自函數運算。在陳炯堯(1997)的先前研究中，腦波依據取樣頻率規則， α 波以100Hz的取樣頻率； β 波以500Hz取樣進行A/D轉換後，再送入電腦進行腦波自函數的有效時間(τ_e)之數值計算(圖 2-3)。另外在陳炯堯、詹曼憲(2006)語音之連續自函數運算(τ_e)值計算中，單音節語音最佳積分時間(2T)以0.3s最為有效。而本研究所播放之語音因含有第一反遲延時間之模擬，故調整積分時間(2T)長度為0.5s進行計算。如圖 2-3所示，在相同第一反遲延時間設定下， α 波與 β 波自函數波形具相當程度之差異。反之，不同空間第一反射遲延時間情形下單音節語音之自函數並無太大差異。

在腦波記錄部份，於朝陽科技大學半無響室中，8名受測者坐在可以保持舒服姿勢的辦公椅上接受腦波誘導與記錄；溫控在 $22 \pm 2^\circ\text{C}$ ，於實驗之前接受左右腦使用的基本調查，確認受測者均無左撇子。並禁止腦波記錄一週內飲酒，於一小時內禁止吸煙。而腦波探測電極位置則依照國際10-20系統連接於受測者頭顱T3及T4部分。參考電位為兩側之耳墜部份，進行左、右腦之連續腦波的單極誘導。而以G2連結於眉心作為眼動參考電極。每次進行腦波記錄時，都將電器系統進行接地的動作，以避免外在之電氣干擾。模擬聲場之配置如前述心理實驗之設定。將所收集的腦波資料經由NI LabVIEW軟體進行分析處理，並同時針對眨眼動作進行偵查，去除它對腦波的影響(ocular artifact reduction)。

在主觀聲源寬廣度的感知改變影響下，以相同於心理實驗的9位受測者的腦波同期誘導結果來進行記錄與分析。然而，在腦波觀察方式上，由於音訊空間印象屬於短時間的記憶現象，在微弱的腦波訊號反應上通常利用大腦誘發強度(auditory evoked potential, AEP)的波形來觀察其變化。而對於這種由音刺激開始到500ms內的快速反應通常以訊號平均法(Ichikawa, 1983)來取得一致且明顯之腦波波形。且波形的振幅(amplitude)與波峰、波谷的時間位置之移動(潛時, latency)也可反應聽覺神經不同部位活化的象徵。如圖 2-4 所示，本研究是以固定之反射聲遲延與迴響時間($\Delta t_1 < 15.5 \text{ ms}$, $RT \neq 0.1 \text{ s}$)與不同到來方位及能量(表 2-3)來改變聲場對聲源寬廣度的心理感知改變。本研究假設腦波由於前述時間參數設定反應時間當大於10ms，在波形觀察是以慢性頭頂反應(slow vertex responses, SVR)來進行。藉此取得聽覺誘發電位(AEP)後段部份波形(30~200ms)之P1、P2、N1、N2電位在受到聲音訊號刺激時P1-N1、P2-N2彼此間振幅差與P1、P2、N1、N2之潛時的變化特性。

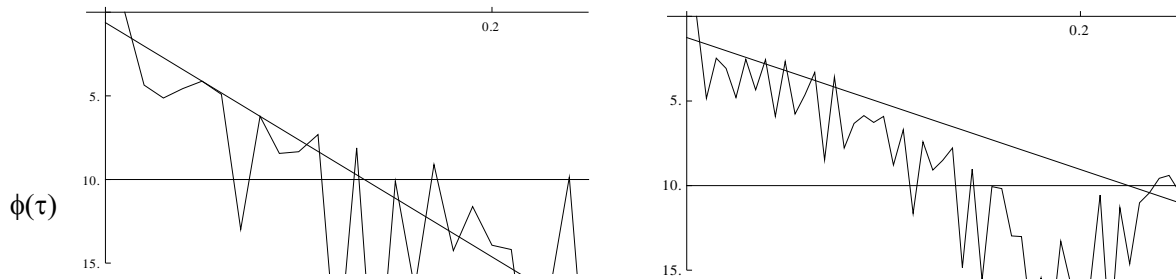
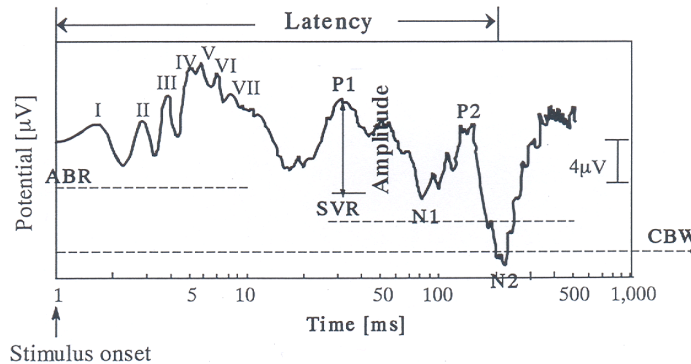
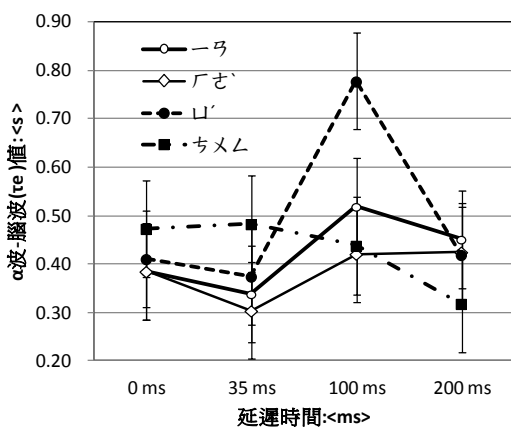
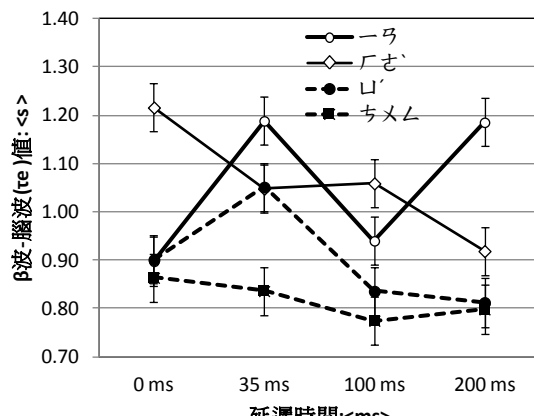
圖 2-3 單音節語音「ちメム」於聆聽時所記錄腦波 α 波(左)與 β 波(右)自函數之計算結果

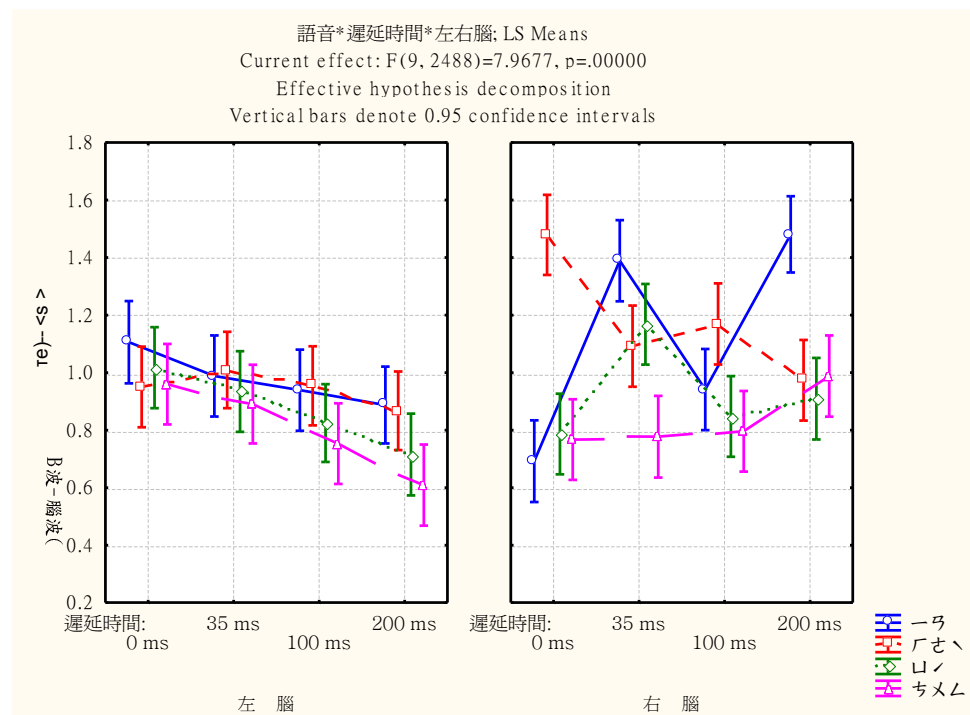
圖 2-4 Ichikawa 等(1983)所建立之大腦誘發強度(AEP)各部之定義圖說

3 實驗結果與討論

3-1 語音清晰度對腦波之影響

第一反射遲延時間改變下單音節語音對於 α 波與 β 波都有明顯差異性， α 波 ($F=12.96(9, 2488)$, $p<0.001$)、 β 波 ($F(9, 2488)=5.21$, $p<0.001$)。由圖 3-1 與 3-2 得知，右腦記錄所得 β 波之自函數明顯與主觀心理的語音清晰度有正相關之關連性。然而 α 波部份腦波反應除語音「ちメム」之外，其餘都在 100ms 處呈現增加趨勢。此結果是否與鼻音發音有密切關係在此無法證明，但就心理實驗結果可知 4 個語音中以 100ms 之反射遲延得到最低之正答率。而「ノ」、「カ」與「ヲ」之結果又恰與正答率趨勢相反。此處 100ms 又與 Ando (1985) 在聲場喜好研究中提出之不快反射遲延的 135ms 最為接近 (echo disturbance)。因此 α 波是否確實反映了聲場對反射遲延時間的不悅感，確實令我們矚目。

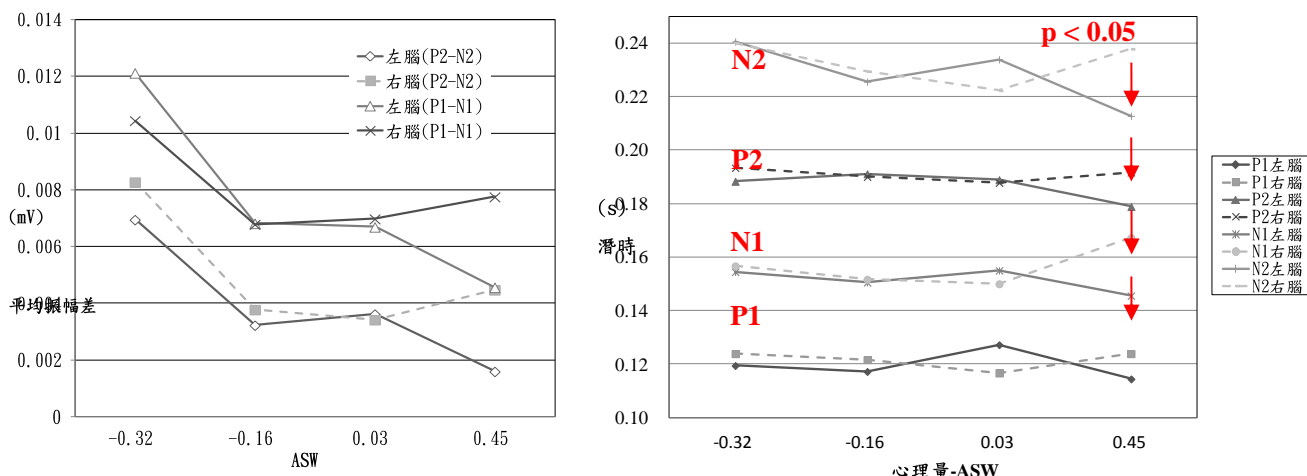
圖 3-1 左腦 α 波對於遲延時間與單音節語音關係圖圖 3-2 右腦 β 波對於遲延時間與單音節語音關係圖

圖 3-3 β 波在空間反射遲延時間影響下對單音節語音之左、右腦波反應

在 β 波的變化中，由圖 3-3 得知左腦對於空間反射遲延時間影響結果非常一致($F(9, 2488)=5.21, p<0.001$)，但對語音間心理反應之先後順序並無顯著差異，其差異反而在右腦顯著得到。因此左右腦 β 波的變化在空間反射遲延時間與語音間心理反應分別出現於左與右腦。

3-2 主觀聲源寬廣度的感知與腦波變化

在實驗中，9位受測者之大腦誘發電位後期慢性頭頂反應(SVR)之結果如圖 3-4 顯示，在左腦部份 SVR 振幅差與心理量化值趨勢成一致反比趨勢($p<0.05$)。但由於 ASW(-0.16)與 ASW(0.03)之間心理差異不大而難有明顯結果。



然而在左右腦的潛時變化部份發現，僅於左腦 N2 位置出現 ASW(0.03)與 ASW(0.45)之間的有效差異($p < 0.05$)。而趨勢上 ASW(0.45)潛時均小於 ASW(0.03)潛時是可由圖 3-5 中左腦的一致性被察覺出來；而右腦 ASW(0.45)潛時均大於 ASW(0.03)潛時也是一致的。以上結果可發現振幅差表現於左腦是主觀聲源寬廣度影響受測者對聲場喜好所導致；而潛時於 N2 部位的一致性是神經部位活化的特徵。且均明顯發現於 ASW(0.03)與 ASW(0.45)之間。即明顯出現於 IACC = 0.56 與 0.68 之間。這反應大腦對此改變與 IACC 的極值 0.35 與 0.81 並無太大影響，與圖 2-2 之心理反應結果一致。

4 結論

就以上兩組腦波實驗之設計與結果發現，單純之聲場物理條件變化與複雜之心理回饋影響大腦腦波反應時，左右大腦專門化理論的表現結果變得異常複雜。基本上本研究根據聲場喜好程度不論在時間或空間物理量上偏向於左腦被活化；而當受測者是以判斷角色記錄腦波時，右腦腦部活化較趨近判別之對象。如本研究在語音清晰度研究上以連續腦波(CBW)進行觀察時，對於聲場第一反射遲延的反應於左腦甚為明顯(圖 3-3)。而語音之清晰程度卻是反應自右腦的複雜思考(即腦部回饋行為)。這點在主觀聲源寬廣度影響實驗上獲得證實，對於空間物理因子之變遷，IACC 值改變下依舊在左腦得到聲場改變的情報。而右腦對於較為明顯之主觀聲源寬廣度變化(ASW(0.03) 與 ASW(0.45)) 却同時存在於左右兩側。在心理學上集中注意(focus)與情境感知(ambient)的兩種腦部使用方式所激活的腦波活化部位完全不同。而大腦半球專門化問題決定於集中意識之結論是多見的，如 Floel et al. (2005) 利用空間視覺集中實驗在 Doppler 超音波裝置上透過核磁共振(MRI)設備觀察正常右手撇的受測者大腦反應，發現空間辨識與言語功能均活化於右腦的臨床實驗結果。

參考文獻

- [1] 楊良治，(1997)，心理實驗綱要，五南圖書出版有限公司，台北市。
- [2] 陳炯堯、壽田喜治、安藤四一，“聲場中持續變動之腦波解析:左右大腦皮質alpha波之互函”，第二十屆學術研討會，中華民國音響學會，台北，(1999)。
- [3] 張淳華，「雙耳互函數與聲源方向感度之探討—以兩反射音模擬聲場為例」，碩士論文，朝陽科技大學建築及都市設計研究所，台中市，(2000)。
- [4] 簡佑宏，”運用腦波測量儀器測聽情緒反應中原學報”，第三十三卷第一期，(2006)
- [5] 游財榮，「中西傳統樂器獨奏時之主觀聲源寬廣度比較研究」，碩士論文，朝陽科技大學建築及都市設計研究所，台中市，(2009)。
- [6] 陳永祥，「空間語音清晰度與大腦皮質上連續腦波之關聯性」，碩士論文，朝陽科技大學建築及都市設計研究所，台中市，(2010)。
- [7] 林威宇，「單音節語音聽取明瞭度與室內雙耳互函數之關聯性研究」，碩士論文，朝陽科技大學建築及都市設計研究所，台中市，(2011)。
- [8] Akita ,T. , Fujii, T., Hirate, K. and Yasuoka, M., A research on auditory information processing in the brain when a person at his task by eans of measurement and analysis of auditory evoked potential, J. Archi. Plann. Environ. Engng.AIJ , (1998) .
- [9] Ando,Y..Concert Hall Acoustics, Berlin Heidelberg ,New York , (1985)
- [10] Ando,Y. and Kurihara, Y., Nonlinear response in evaluating the subjective diffuseness of sound fields, J. Acoust. Soc. Am., 80(3), (pp. 833-836) . (1986) .
- [11] Ando, Y., Kang, S. H., & Morita, K., On the Relationship between Auditory-Evoked Potential and Subjective Preference for Sound Field, J. Acoust. Soc. Jpn. (E), 8. (pp.197-204) . (1987)
- [12] Ando, Y., Kang, S. H., & Nagamatsu, H., “On the Auditory-Evoked Potential in Relation to the IACC of Sound Field,” J. Acoust. Soc. Jpn. (E), 8 (pp.183-190) . (1987)
- [13] Ando, Y., Important Subjective Attributes for the Sound Field, Based on the Model, Architectural Acoustics, Blending Sound Sources, Sound Fields, and Listeners, (pp.89- 95) . (1996)
- [14] Beranek, L. Concert Hall Acoustics, J. Acoust. Soc. Am., 85, (pp. 39) . (1992)
- [15] Damaske, P., Diffuse onset of reverberation, *Music & Concert Hall Acoustics*, Conference Proceedings From MCHA, (pp.171-182) . (1995)
- [16] Ichikawa, G., et al, The Logarithmical Presentation for Auditory Evoked Potential, *Audiology Jpn.*, 26(pp. 735-739) . (1983)
- [17] Jasper, H. H., The 10/20 Electrode System of the International Federation, *Electroenceph. Clin. Neurophysiol.*, 10 (pp.371 - 375) . (1958)
- [18] Morimoto, M. and Posselt, C. Contribution of reverberation to auditory spaciousness in concert halls, J. Acoust. Soc. Jpn (E) 10, (pp.87-91) . (1989)
- [19] Morimoto, M. and Iida, K., “A practical evaluation method of auditory source width in concert halls,” J.Acoust. Soc. Jpn. (E) 16, (pp.59-69) . (1995)
- [20] Sato, S., Mori, Y., and Ando, Y., The subjective evaluation of source locations on the stage by listeners, *Music & Concert Hall Acoustics*, Conference Proceedings From MCHA, (pp.117-123) . (1995)
- [21] Sato, S., and Ando, Y., Intramural Cross-Correlation Function on Subjective Attributes , J. Acoust. Soc. Am, 100(A) , (pp. 2592) . (1996)
- [22] Schmidt, R. A., and Wrisberg, C. A., Motor learning and performance: A problem-based learning approach, (2nd ed.), Champaign , IL: Human Kinetics. (2000)
- [23] Thurstone, L. L. Psychol. Rev, 34, (pp.273-289) . (1927)
- [24] Floel, A., Jansen, A., Deppe, M., Kanowski, M., Konrad, C., Sommer, J. and Knecht, S., “Atypical hemispheric dominance for attention: functional MRI topography,” J. Cerebral Blood Flow & Metabolism, 25, (pp.1197-1208) . (2005)

上海梅塞德斯-奔驰文化中心建声设计研究

Architecture Acoustics Design & Research for Shanghai Mercedes-Benz Arena

张晓岚

ZHANG Xiaolan

(章奎生声学设计研究所)

(Zhang Kuisheng Acoustic Design & Research Studio, Shanghai, PRC)

Abstract: This paper introduces the Shanghai Mercedes-Benz Arena, especially the architecture acoustics design.

Key words: Shanghai Mercedes-Benz Arena; Architecture acoustics design; Multi-purpose hall design

摘要: 本文对上海梅塞德斯-奔驰文化中心（原上海世博文化中心）从建筑、声学、使用等几个角度进行介绍，其中特别着重建筑声学设计研究过程。

关键词: 上海梅塞德斯-奔驰文化中心；建筑声学设计；多用途场馆设计

1 概述^[1, 2, 3, 4, 5]

上海梅赛德斯-奔驰文化中心（原世博演艺中心）是中国上海 2010 年世博会“一轴四馆”五个永久性建筑之一。位居世博轴以东核心区重要区位；西侧与庆典广场相连，并与世博中心相呼应；北临黄浦江，与世博浦西园区隔江相望，东侧为保留的成品码头和滨江绿带。

奔驰文化中心建设投资约 20 多亿人民币，用地面积 67,242.6 平方米，总建筑面积 140,277 平方米。其外形呈飞碟型，寓意“时空飞梭”，已经成为上海浦东黄浦江边的一座地标性建筑。

奔驰文化中心集文化、娱乐、餐饮等多种功能为一身。其中包含一座最多可容纳 18,000 人的多功能可变容座规模主场馆，一座音乐俱乐部、一座真冰滑冰场、多厅电影院以及众多知名餐饮、购物场所，可以让市民在此自由选择，轻松度过一段愉快的时光。

奔驰文化中心中的核心场馆为 18000 座多功能可变场馆。该场馆不同于普通的体育场馆或观演场所。首先，该场馆可以根据具体的使用情况灵活变化其可容纳的观众人数。容座可在 18000、12000、8000、5000 四种条件中变化。其次，该场馆既可以作为大型歌舞、演唱会的表演场所，又可以作为冰球、NBA 篮球等体育赛事的赛场。使用功能多用途。第三，场馆可以根据具体观众人数、使用功能，灵活的改变舞台和观众的关系。舞台形式可以从岛式舞台到尽端式舞台灵活变换。第四，为了配合不同使用条件、观众人数以及克服场馆内无足够仓储空间的限制条件，该场馆建筑设计主创人员与座椅供货厂商共同研发了视线可调节座椅系统，成功达到一套座椅系统可以满足多种使用要求。此做法在国内尚属首创。第五，主场馆内部体积巨大，高达 272000 m³，属于超大型观演场馆。但受到建筑、结构实际条件限制，建筑声学设计既要保证场馆内拥有出色的建筑环境，又要使所有的声学措施都满足实际条件。建筑声学设计人员为此付出了很多心血和努力。为保证奔驰文化中心设计顺利进行，上海华东建筑设计院特别向上海市科委申请了专项课题研究，建筑声学设计研究便是其中一个重要的部分。

自 2010 年建成以来，奔驰文化中心主场馆已成功举办多次商业演出。例如王菲演唱会（上海站）、前世界三大男高音之一卡雷拉斯演唱会均选择在文化中心主场馆，并取得了圆满的演出效果。

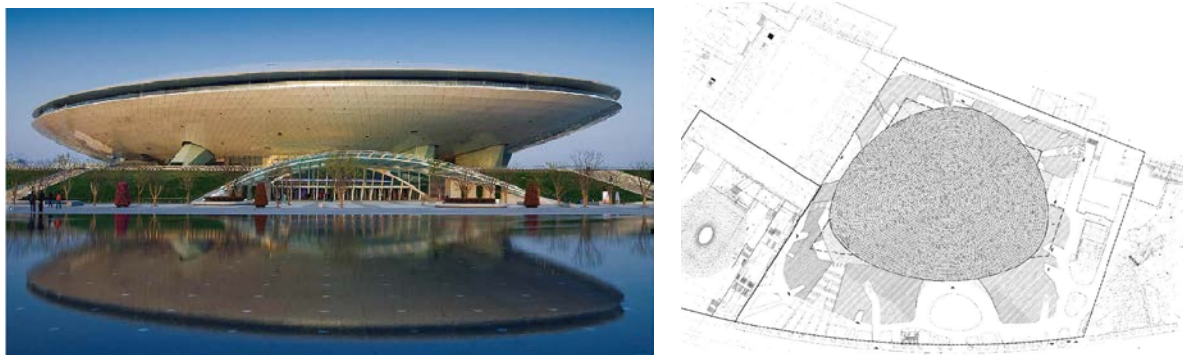
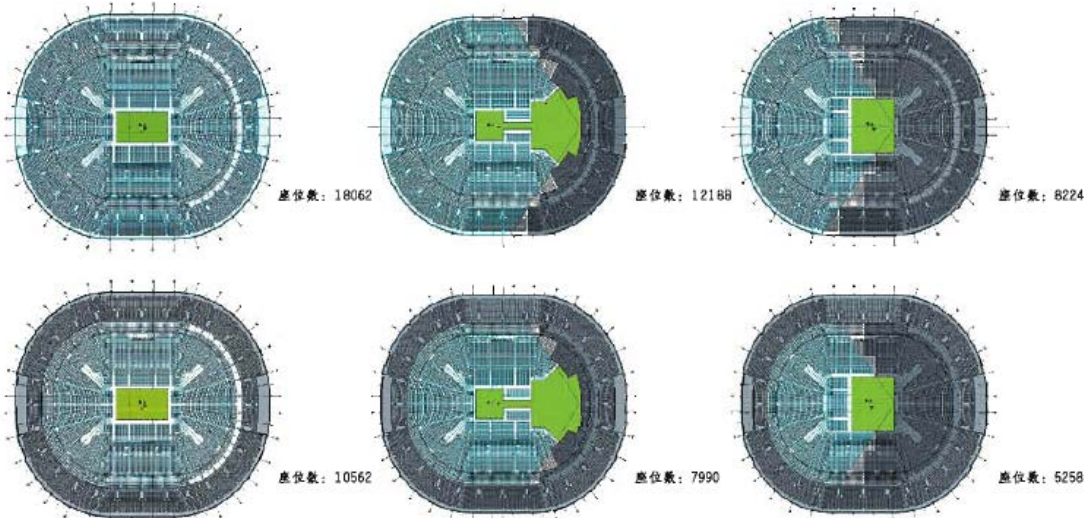


图 1 上海梅塞德斯-奔驰文化中心外景照片和总体平面图



主场馆灵活分隔示意图

图 2 上海梅塞德斯-奔驰文化中心主场馆不同人数和舞台布置示意图

2 主场馆建筑声学设计

2.1 建筑声学设计目标^[6]

奔驰文化中心主场馆为多用途场馆，使用时以电声为主。建筑声学需要为电声营造一个安静、清晰的基础声学环境。

根据国家相关规范声学要求，确定场馆内基本音质（满场条件）参量如下：

1) 根据主场馆的功能定位，本场馆满场条件混响时间：T30=1.8~2.0s。各频率混响时间要求如表 1.

表 1 各频率混响时间设计要求：

频率 (Hz)	125	250	500	1000	2000	4000
混响时间范围	2.5~3.0s	2.0~2.5s	1.8~2.0s	1.8~2.0s	1.5~1.8s	1.2~1.8s
混响比值*	1.0~1.3	1.0~1.15	1.0	1.0	0.9~1.0	0.8~1.0

*各频率混响时间与中频 (500Hz) 混响时间比值

2) 在空调正常运行条件下，主场馆空场时，场内背景噪声应达到 NR-35。

3) 场馆内无回声、颤动回声、声聚焦等音质缺陷。

2.2 主场馆不同使用条件声学设计研究^[7]

世博奔驰文化中心主场馆可以通过升降围栏的分隔方式，将 18000 座场馆分成为 12000 座、8000 座、

5000 座等多种容座条件。分隔后，场馆内观众分布将集中在场馆一侧，观众分布不均匀。分隔用栏板材料的选择，栏板规格的选择都成为了需要研究的重点内容。

建筑声学设计利用计算机模拟软件 CATT，模拟研究主场馆内应用不同分隔隔板材料、隔板规格后的声场情况。在建筑声学计算机软件 CATT 中为主场馆的四种不同分隔方式建立了计算模型。以 18000 座条件为场馆的基本模型。在假设多种隔板材质、规格、分隔方式进行模拟计算。通过对模拟结果变化的观察来决定分隔围栏的使用。合理的围栏应该既能保证声场质量，又可以满足建筑的需求。

模拟计算中共选用了 3 种不同材质作为围栏的备选方案。通过对不同情况的大量模拟计算与模拟结果的对比研究。

条件 1：低吸声系数、高透声系数的材质，例如：普通的布、纱幕；

条件 2：高吸声系数、高透声系数的材料，例如：吸声帘幕；

条件 3：高吸声系数、低透声系数的材料，例如：表面进行吸声处理的轻质板材。

通过对比，认为条件 2 中材质的围栏对控制声场内混响时间最为有利。但在实际操作中，由于长达十几米的厚分隔围栏材质在收纳时会占用过大的空间，而且顶部荷载也无法支撑，与建筑实际情况有冲突。条件 1 和条件 3 在模拟结果上相差较小，条件 1 的混响时间模拟结果更低，且在使用中条件 1 比条件 3 更简便。故在实际使用中，条件 1 的材质为最合理选择。

在实际项目中，围栏材质上部为软帘，与观众较为接近的下部为较硬质的分割板。这样既可以有效地对场地进行划分，又兼顾了声学效果，一举两得。

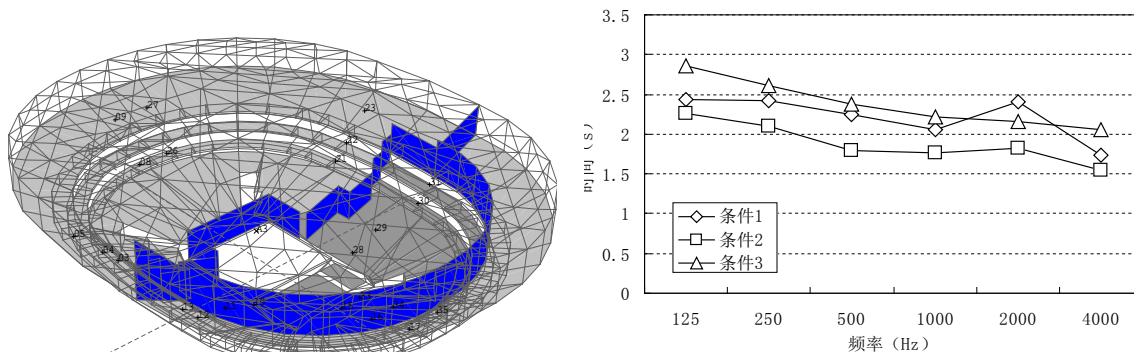


图 3 CATT 模型与 3 种条件混响时间模拟结果示意图。

2.3 主场馆混响时间控制

场馆内体量大，且体型扁平。侧面墙面积占总表面积比例小，顶部要求吊装大量马道、音视频、灯光等设备，挑台等位置还需要按照 LED 等装置。故可以进行声学吸声处理的空间、面积有限。声学也无法使用传统空间吸声体等手段来控制场馆内声学效果。这些从图 4 中均可得到一定程度的体现。

建声设计的关键点和难点就在于如何：1) 如何最大程度地利用场馆内有限地面积进行声学处理；2) 如何将声学处理隐藏在主场馆的室内装修之中。

过于庞大的体积导致主场馆内声场无法达到充分扩散，因此单纯使用经典理论公式计算得到的场馆内音质参数可能会与未来的实际情况存在较大偏差。为了避免这种偏差而对设计带来失误，声学对主场馆建立模型，使用计算机模拟软件 Odeon 对主场馆进行声学模拟，分析主场馆中混响时间变化。

经过反复模拟计算，主场馆需要在顶部、大面积侧墙均采用吸声处理的前提下，才可达到预期的设计目标。主场馆顶面使用吸声屋面做法，而墙面则以中高频吸声做法为主。

模型内材料布置大致设定：

表 2 主场馆内部声学材料布置

位置	材料布置
屋盖	吸声材质，采用保温、隔声、吸声轻质屋面*
观众席后墙	穿孔板吸声做法与织物软包吸声板做法结合
挑台栏板	LED 显示屏、广告
挑台吊顶	石膏板，外刷涂料

*屋面构造见图 5。

模拟计算结果如表 3 所示，基本满足声学设计要求。

表 3 主场馆混响时间模拟结果（满场按 18000 人计算）

频率	125Hz	250Hz	500Hz	1KHz	2KHz	4KHz
RT(空场)	3.38s	2.68s	2.29s	2.16s	2.03s	1.67s
RT(满场)	2.88s	2.21s	1.93s	1.87s	1.78s	1.46s

为了保证建筑声学环境不会发生因观众人数不同而发生大的变化，声学要求座椅选择时要尽量选择满场、空场吸声量相近的产品。

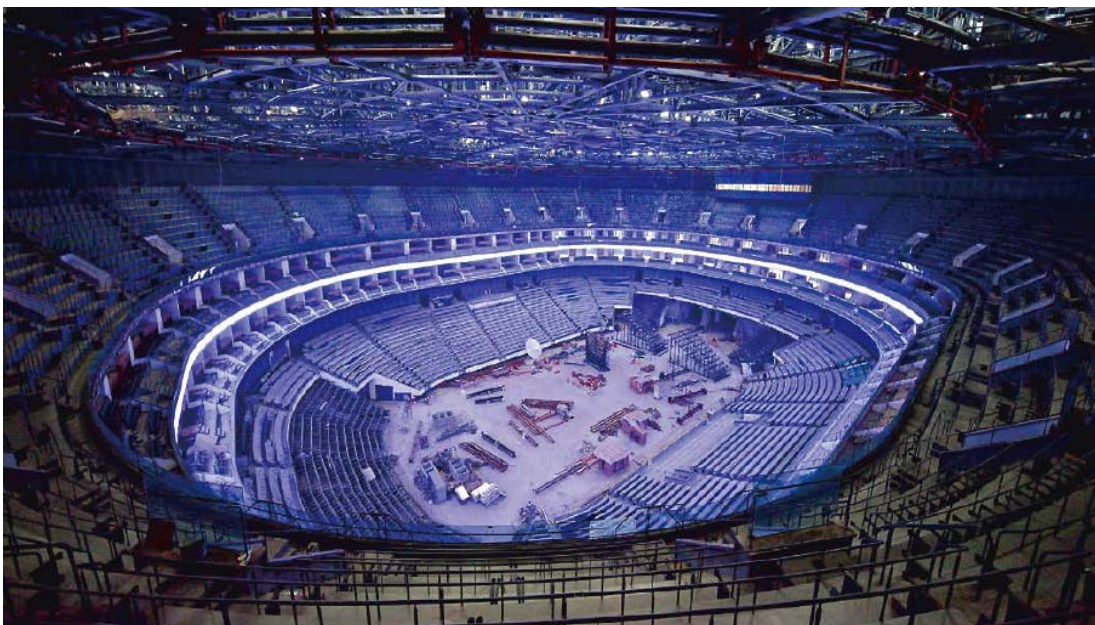


图 4 建设中的奔驰文化中心^[5]

2.4 主场馆内背景噪声控制

主场馆内的噪声主要来自屋面的雨水撞击、周围临近的设备机房、场馆内的空调系统。

2.4.1 隔绝屋面雨水撞击噪声

经过声学与建筑专业的共同研究，在瑞士贝姆屋面系统的基础上，研发了更适合文化中心主场馆的声学屋面。该屋面在屋面的隔声性和外观装饰性上都有更优表现。

主场馆屋面系统主要有三部分构成：

- a) 最外层使用 20mm 厚蜂窝装饰板来替代常规的铝单板或合金板。蜂窝板强度高于常规使用的铝单板或者合金板，因此其可以最大限度地减少雨水撞击噪声。对于屋面系统而言，雨水撞击噪声是最主要的噪声源。
- b) 中间部分为隔声层，其构成为：0.9mm厚直立锁边屋面板（合金板）+100mm厚保温岩棉（密度为 100kg/m³）+2mm厚镀锌钢板。
- c) 最外层与中间隔声层之间保留一定厚度的空腔，这样可以增加屋面系统的隔声量。
- d) 最下面部分为吸声层，空腔+50mm厚离心玻璃棉（密度为 100kg/m³）+无纺布+0.7mm厚穿孔压型钢板（穿孔率约 20%）。

与其它声学屋面相比，文化中心主场馆声学屋面加强了最外层板材的厚度和强度，同时最外层外面与中心隔声层之间留有 30~40cm 的空腔，提高了隔绝噪声的能力。另外，屋面的吸声层也优化了穿孔率，提高了屋面的吸声性能，使屋面在低、中、高各频段都保持较高的吸声量。

根据工程经验预测，主场馆屋面系统的隔声量可达 50dB 以上。

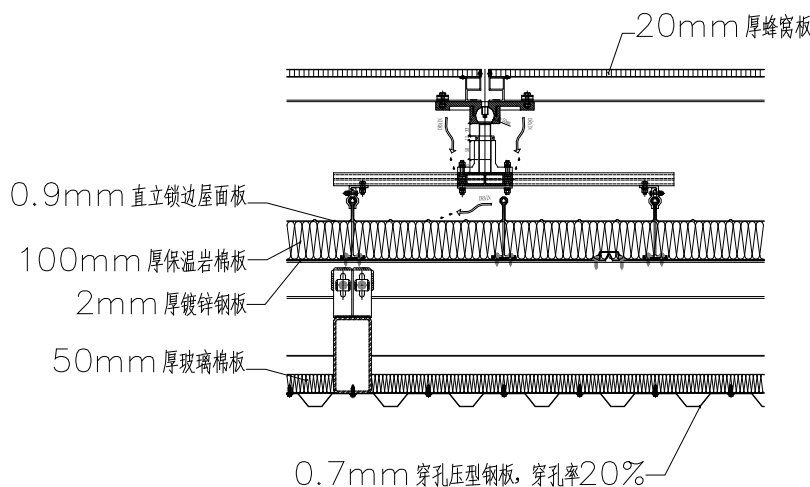


图 5 奔驰文化中心主场馆屋面构造

2.4.2 隔绝周围临近设备机房噪声

受到场地限制，奔驰文化中心采用了下小上大的建筑体型，这样也带来了场馆上部荷载限制。根据建筑要求，场馆在标高 11m 以上区域墙体全部必须使用轻钢龙骨石膏板轻质墙体构造。因此，高区设备机房噪声控制的控制要点主要体现在

- 1) 合理布局机房位置，尽量让机房远离有安静要求房间；
- 2) 选用噪声较小的设备机组，并做好设备的振动控制工作；
- 3) 严格监督轻钢龙骨石膏板轻质墙体施工，确保墙体隔声量达到要求。

2.4.3 控制空调系统风噪声

根据设计要求，主场馆内背景噪声不应超过 NR-35 曲线。根据此要求，空调系统中各部分风速应控制在下表范围之内：

背景噪声评价标准	管道内气流速度的允许值 (m/s)		
	主风管	次风管	房间出风口
40dBA	≤ 7.5	≤ 6.0	≤ 4.0

建筑声学设计中还需对主场馆风管系统中噪声控制最不利管线进行消声控制计算，合理布置消声器的位置和数量。

2.5 主场馆使用效果

由于世博期间安保限制，奔驰文化中心主场馆建成后无法及时安排现场声学测量。而世博后，由于管理人员更换以及演出密集等原因，一直无法安排实地测量。因此非常遗憾的是，本场馆并没有实测数据来评价主场馆的声学状况。根据现场演出时听闻，主场馆内声音清晰，主观听音估计为 1.8~1.9s，复核设计预期要求。其音质效果也获得业主单位和一些演出使用单位的好评。

3 结论

梅塞德斯-奔驰文化中心自建成后已成功举办多场商业演出，演出类型从大型话剧、晚会到演唱会。2012 年已正式被提名为上海场馆 5 强。项目本身也先后获得全国以及上海市勘察设计行业协会 2011 年度优秀工程设计一等奖。其科研项目“超大型综合观演建筑设计技术研究”也获得上海现代建筑设计（集团）科技进步奖一等奖。

“时空飞梭”梅塞德斯-奔驰文化中心无疑已成为上海市民休闲娱乐的好去处，上海城市一座时尚的城市坐标。

參考文献

- [1] 汪孝安, 魯超, 田園, 涂宗豫, 面向未來 2010 上海世博會世博演藝中心《時代建築》, 2009-4, 48-53
- [2] 傅海聰, 上海演藝建築的多元化發展, 《演藝科技》, 2011 年第十期 总第 63 期
- [3] 世博文化中心, 建設科技, 低碳世博——中國 2010 年上海世博會特刊, 64-71.
- [4] 世博演藝中心: 时尚新地标 文/上海市城建檔案館, 1994-2012 China Academic Journal Electronic Publishing House
- [5] 借天不借地, 在限制中設計——世博文化中心, 《現代建築技術》, 92-115, 2010-4, 总第 48 期
- [6] 《體育建築設計規範》, JGJ-31-2003, 2003-5-3 發布
- [7] 張曉嵐 章奎生, 上海世博文化中心主場館建築聲學設計, 《演藝科技》, 2010 年總第 52 期, 109-113

厅堂侧墙体型设计对厅内混响时间影响的研究

Research on the influence of bodily form design of side wall of a hall to its reverberation time

杨小军

YANG Xiaojun

(上海现代建筑设计(集团)有限公司 章奎生声学设计研究所 200041)

(Shanghai Xian Dai Architectural Design (group) Co. Ltd Zhang Kuisheng Acoustic Design Institute 200041)

Abstract: Reverberation time is a very important parameter of architectural acoustics design. In the classical theory of architectural acoustics, reverberation time of a hall relates to its cubage, total inner surface area and average absorption coefficient and has nothing to with the idiographic bodily form of the hall. In sound quality design of two different halls, reverberation time of each may be similar according to classical theory while the spot measurement results are quite different. So it is necessary to research the influence of other factors to reverberation time of a hall. This article mainly researches the influence of bodily form design to the reverberation time of a hall. And under the premise of calculated reverberation time keeps invariable, watch the change of reverberation time to research the influence of bodily form design to the reverberation time through the change of bodily form of part of wall.

Key words: bodily form design; reverberation time

摘要：混响时间是建筑声学设计中非常重要的参量。在经典建筑声学理论中，厅内的混响时间只与厅内容积、内表面积、平均吸声系数等因素有关，与厅堂内部具体的体型无关。在厅堂音质设计时会遇到，两个厅堂根据经典混响时间计算公式算得的混响时间差不多，但是实际测量的结果却相差很大。因此有必要研究其他因素对厅内混响时间的影响。本文着重研究了厅堂体型对厅内混响时间的影响。在保证混响时间公式计算结果不变的条件下，通过改变厅堂内部部分墙面的体型，观察厅内混响时间的变化情况，来研究厅堂体型变化对厅内混响时间的影响。

关键词：体型设计；混响时间

1 引言

混响时间是厅堂声学音质评价的重要指标，同时也是建筑声学设计的重要参量。经典的建筑声学理论中，混响时间的计算公式是在扩散场的假设下推导出来的，理论上说厅内的混响时间只与厅的容积、内表面积、平均吸声系数等因素有关，而与厅堂内部具体的体型无关。在厅堂音质设计时会遇到，两个厅堂根据经典混响时间计算公式算得的混响时间差不多，但是实际测量得到的结果却相差很大，因此有必要研究其他因素对厅内混响时间的影响，本文着重研究了厅堂的侧墙体型对厅内混响时间的影响。在保证厅内的混响时间按照公式计算的结果保持不变的前提下，通过改变厅堂部分侧墙墙体的体型，观察厅内混响时间的变化情况来研究厅堂体型对厅内混响时间的影响。文中通过建立计算机模型，并采用厅堂声学计算机模拟软件 Odeon 来模拟厅内部分墙体变化时的混响时间。

2 经典混响时间理论

本节主要介绍经典声学理论基础中的平均吸声系数和混响时间等概念^[1]。

2.1 平均吸声系数

声波在厅堂内碰到壁面时，如果壁面并非刚性，它们对声波就会具有一定的吸收能力，这样一部分入射声波就会被壁面吸收，被壁面吸收的能量与入射能量的比值称为壁面的吸声系数 α_i 。由于在扩散声场的条件下声能向各个方向传递的几率是相同的，所以每一吸声表面的入射声在所有方向都具有相同的几率，因此这一吸声系数 α_i 是对所有入射角平均的结果。平均吸声系数是对厅堂内所有的吸声表面进行平均：

$$\bar{\alpha} = \frac{\sum_{i=1}^n \alpha_i S_i}{\sum_{i=1}^n S_i} \quad (1)$$

其中 S_i 为厅堂内某个吸声面的面积。平均吸声系数表示厅堂内壁面单位面积的平均吸声能力，也称为厅内表面的平均吸声系数。如果房间内部除了壁面吸声以外，还有其他的吸声体，如人、坐席等，平均吸声系数可以修正为：

$$\bar{\alpha} = \frac{\sum_{i=1}^n \alpha_i S_i + \sum_{j=1}^m S_j \alpha_j}{\sum_{i=1}^n S_i} \quad (2)$$

上式中的 $S_j \alpha_j$ 为其他吸声体的吸声量。

2.2 混响时间

在厅堂中，从声源发出的声波在传播过程中由于不断经过壁面或者其他物体反射，其声能量被壁面和物体吸收而逐渐衰减。声波在各方向不断地来回反射，而又继续衰减的现象称为室内混响。

混响时间的定义为：在扩散声场中，当声源停止后从初始的声压级降低 60dB（也就是平均声能密度衰减到原来的 $1/10^6$ ）所需的时间，用符号 T_{60} 来表示。

取 $C_0=344\text{m/s}$ ，则可以得到混响时间的表达式：

$$T_{60} = \frac{0.161V}{-S\ln(1-\bar{\alpha}) + 4mV} \quad (3)$$

其中 V 为房间体积，单位：立方米； S 为房间内表总面积，单位：平方米； $\bar{\alpha}$ 为室内平均吸声系数， m 为空气的声强吸收系数。

3 厅堂模型及模拟条件

本节主要介绍所模拟的厅堂模型以及经过调整后得到的不同体型的模型，并且对模型在计算机模拟时的声源、厅堂内壁面材料吸声系数、模拟网格面等声学条件做了说明。

用于研究的厅堂的模型如下图（1）所示，图中红色墙体为侧墙面的调整部分。

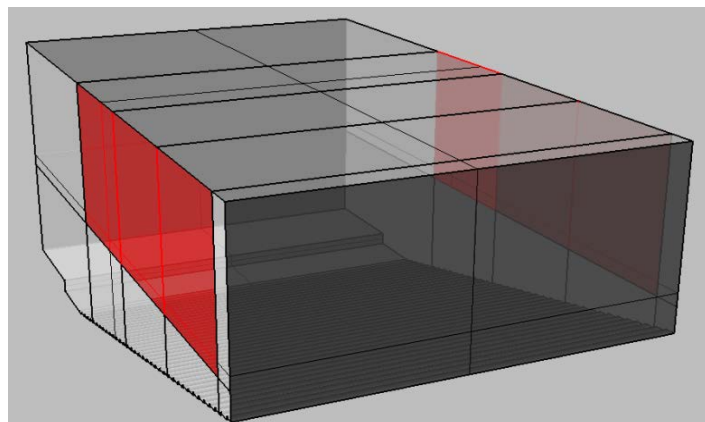


图 1 研究的厅堂模型

将模型中调整部分的墙体分成三块相同的调整块，每块调整快在调整过程中分别按照竖直中心轴旋转和水平中心轴翻转得到不同的厅堂体型。调整墙旋转或者翻转的过程中，厅堂的总容积始终保持不变，内表面积会略微增加，但增加的内表面的吸声系数很小，因此在调整过程中依据混响时间计算公式得出的厅内的混响时间将能保持不变。调整墙旋转和翻转时厅堂的模型如图 2 和图 3 所示，图中 0° 表示原模型：

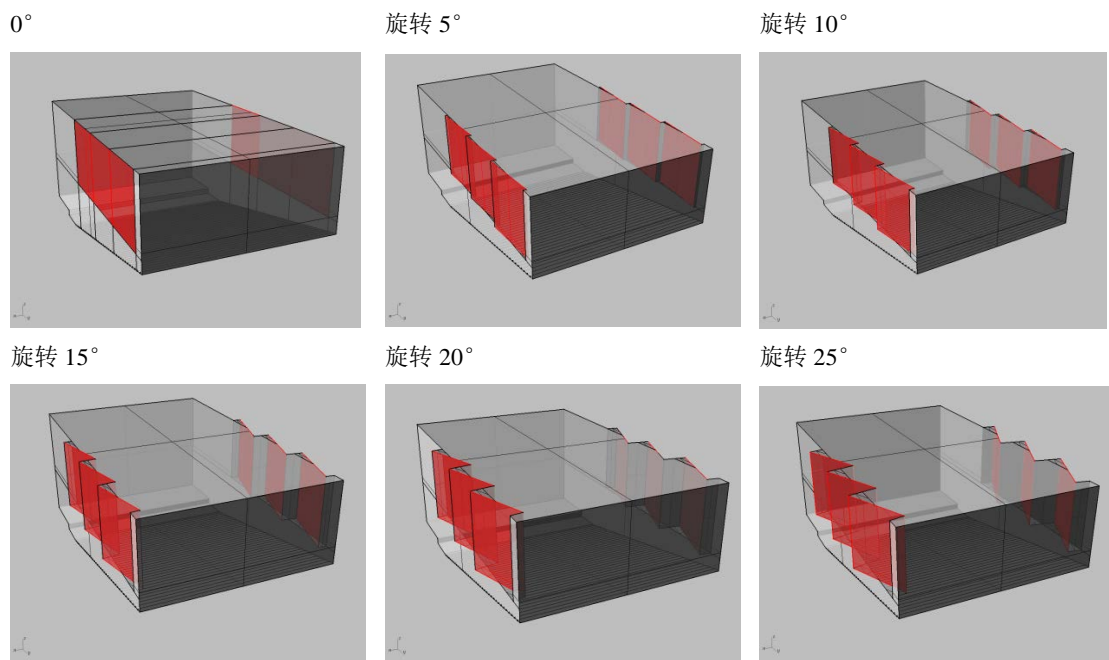


图 2 调整墙旋转时厅堂的模型

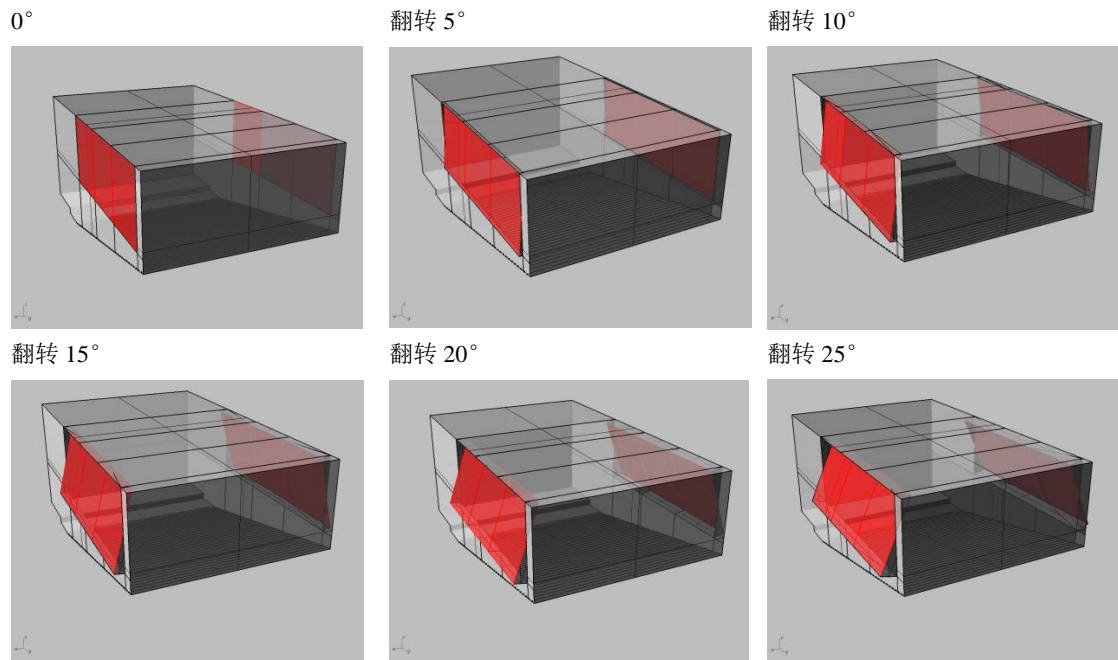


图 3 调整墙翻转时厅堂的模型

模型中的声源选择全指向性点声源，声源置于舞台上且高于舞台面 1.5 米以模拟人说话时发声的高度，声源位置如图 4 所示：

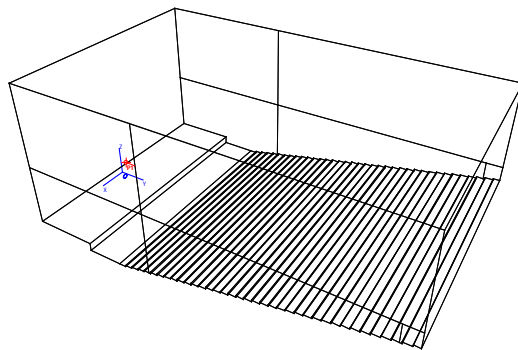


图 4 模型中声源位置

在模拟时，选取的声学模拟网格面为整个坐席区域的正上方且高出坐席区域 1.2 米用以模拟坐席区人耳的高度，声学模拟网格面的精度选择为 1 米×1 米。模拟时声学模拟网格面分布如图 5 所示：

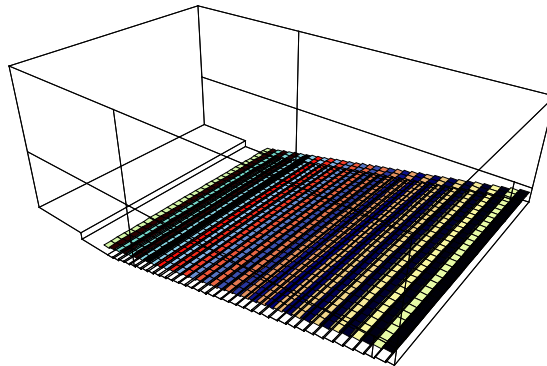


图 5 模拟时声学模拟网格面分布

厅堂模型各内壁面的吸声系数如表 1 所示：

表 1：厅堂模型各内壁面的吸声系数

频率/Hz 内壁面 \	125	250	500	1000	2000	4000
墙面	0.09	0.07	0.06	0.05	0.04	0.03
顶面	0.10	0.08	0.06	0.06	0.04	0.03
地面	0.08	0.06	0.05	0.05	0.04	0.04
台口	0.30	0.35	0.40	0.45	0.50	0.50
坐席区	0.58	0.66	0.70	0.72	0.73	0.73

4 模拟结果及分析

对不同状态的厅堂模型进行计算机模拟，所得到的模拟网格面上混响时间模拟结果的平均值如表 2 所示：

表 2：不同状态下模拟网格上平均的混响时间 T_{30}/s

频率/Hz 状态 \	125	250	500	1000	2000	4000
0° (不动)	3.34	3.36	3.39	3.34	3.13	2.28
旋转 5°	3.87	3.74	3.77	3.57	3.30	2.35
旋转 10°	3.49	3.58	3.59	3.52	3.22	2.31
旋转 15°	3.46	3.48	3.48	3.40	3.19	2.33
旋转 20°	3.61	3.65	3.62	3.53	3.23	2.32

旋转 25°	3.41	3.41	3.42	3.32	3.09	2.32
翻转 5°	3.30	3.36	3.37	3.29	3.15	2.45
翻转 10°	3.20	3.26	3.28	3.21	3.07	2.37
翻转 15°	3.08	3.09	3.10	3.03	2.90	2.29
翻转 20°	3.05	3.06	3.07	2.98	2.85	2.28
翻转 25°	2.95	2.95	2.95	2.86	2.76	2.21

根据上表中的模拟结果，将模拟结果分析比较如图 6 和图 7 所示：

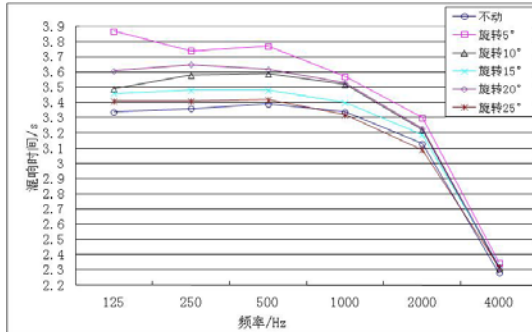


图 6 调整侧墙旋转不同角度时混响时间的均值

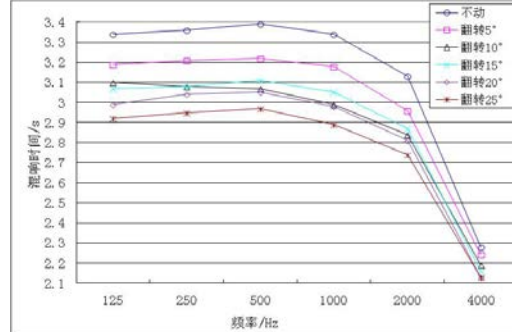


图 7 调整侧墙翻转不同角度时混响时间的均值

从图 6 中可以看出，调整侧墙旋转时，模型中模拟得到的混响时间的平均值没有明显的变化趋势。从图 7 中可以看出：调整侧墙翻转时，模型中模拟得到的混响时间各个频段的平均值基本上有这样的变化趋势：当翻转的角度逐渐增加时模拟的混响时间均值逐渐减小。

从以上两图及其对比的情况我们可以得出：(1) 无论是旋转变化或是翻转变化，对混响时间的影响都是低频相对明显，高频变化偏小；(2) 当侧墙的部分墙面沿着竖直方向的轴朝着观众厅前部旋转时，厅堂内的混响时间将会没有趋势的变化，而当侧墙的部分墙面沿着水平方向的轴朝着坐席区向下翻转时，厅堂内的混响时间将逐渐减小。

5 总结和展望

本文着重研究了厅堂侧墙体型对厅内混响时间的影响。对厅堂侧墙部分墙面的调整得到厅堂不同的体型。通过对不同侧墙体型的厅堂进行计算机模拟得到厅内的平均混响时间。对得到的不同体型下的混响时间的对比分析研究了厅堂体型对厅内混响时间的影响。

对于厅堂体型对厅内混响时间的影响还有很多可以研究，目前的研究只是得出了定性的结论，还没有定量的研究成果，希望能够进行定量的研究，能更好地指导厅堂声学设计。

参考文献

- [1] 杜功焕, 朱哲民, 龚秀芬. 声学基础 [M]. 南京: 南京大学出版社, 2001: 418-449

济南大剧院歌剧厅与音乐厅声学缩尺模型试验研究

Acoustic Scale model Testing of Opera Hall and Concert Hall of Jinan Provincial Cultural & Art Center

余斌

YU Bin

(上海现代建筑设计(集团)有限公司章奎生声学设计研究所, 20041)

(Zhangkuisheng Acoustics Design & Research Studio, Shanghai XianDai Architectural Design (Group) Co. Ltd, 200041)

Abstract: To guarantee the acoustic effects of opera hall and concert hall of Jinan Provincial Cultural & Art Center, scale model test was conducted. The materials of physical models are mainly GRG. Small high-frequency omni-directional speaker is for the sound source to generate linear-sweep signal.

Key words: acoustical design; scale model test

摘要: 为预测济南文化中心歌剧厅和音乐厅建成后的音质状况, 对两厅均做了声学缩尺模型试验, 以确保不出现音质缺陷和验证声学设计计算。缩尺模型的主要制作材料为 GRG 板, 墙面和顶面的扩散造型逼真。试验以小型高频无指向性扬声器为测试声源, 线性扫频信号为声源信号。

关键词: 音质设计; 缩尺模型试验

1 引言

正在建筑中的济南文化中心包括 1600 座歌剧厅、1500 座音乐厅、500 座排练厅及相关配套技术用房等。歌剧厅要求适用于歌剧、戏曲和舞剧等多种演出功能。剧院观众厅平面呈矩形, 设品字形舞台; 观众厅总体积约 22200m^3 , 每座容积约 $13.9\text{m}^3/\text{人}$ 。音乐厅也要求满足大型交响音乐会、室内乐、独奏独唱音乐会以及使用扩声系统时的音乐剧等多种演出需要。音乐厅平面呈椭圆形, 演奏台位于中前区, 平面呈扇形; 观众厅总体积约 16950 m^3 , 每座容积约 $11.3\text{ m}^3/\text{人}$ 。

室内声学的复杂性源于声音的波动性, 缩尺模型试验研究是国际国内演艺建筑观众厅音质设计中最接近实际而又最重要的最科学的辅助设计技术手段。为预测大剧院建成后的音质状况, 确保达到满意的音质效果, 本声学所对歌剧厅和音乐厅均做了音质模型试验。

2 试验概况

缩尺音质模型试验首先要科学合理地确定模型的缩尺比例。根据我声学设计研究所的现有测试仪器装备条件, 模型加工制作精度、费用及试验场所条件, 试验研究所需要的频率范围等多方面因素, 确定歌剧厅和音乐厅音质模型均选用 1:20 的缩尺比例。

2.1 模型制作

歌剧厅和音乐厅模型均按纵轴线分两半制作, 并密封拼合而成, 典型的模型照片分别如图 1 和图 2 所示。模型主体的地面、墙面及顶面均由 GRG 板表面打光, 油漆制作。GRG 作为模型制作材料的优点是显而易见的: 可以做任意复杂的造型, 特别是能逼真地再现界面的微扩散造型, 且尺寸控制更为精准。经 1:20 模型内未放置座椅的缩尺模型现场测试, 并由实测混响时间换算得到 GRG 表面的 20kHz 吸声系数约为 0.072。歌剧厅舞台模型用细木工板制作, 局部舞台及内部墙面做吸声处理, 以控制舞台空间的混响时间与观众厅基本接近。



图 1 歌剧厅 1:20 模型内景照片



图 2 音乐厅 1:20 模型内景照片

歌剧厅和音乐厅观众席座椅均按缩尺比例采用PVC板雕刻成型，软垫用织物模拟制作，首先在模型混响室中进行了模型坐席吸声系数的实测试验：测得座席在相当于实物的 1kHz 倍频带单位面积吸声系数为 0.87，单椅吸声量 0.54m^2 。由于混响室和实际厅堂的声场有所区别，吸声系数也会有一定的偏差，因此我们又安排了在 1:20 厅堂缩尺模型中现场测量了座椅的吸声系数。由实测混响时间换算得到模型座席在相当于实物的 1kHz 倍频带单位面积吸声系数为 0.79，介于满场座椅 1kHz 单位面积吸声系数设计值 0.85 和空场座椅单位面积吸声系数设计值 0.71 之间。

2.2 测试系统

模型试验采用数字测试分析系统进行测量，线性调频信号作为声源信号。通过接收信号与声源信号的反卷积获得模型声场的脉冲响应。测试的频率范围为中心频率 20kHz（相当于实物 1kHz）的倍频带。声能衰减曲线由脉冲响应经 Schroeder 反向积分得到，再按空气声吸收的理论先对其进行修正，后对混响时间 RT 和早期衰变时间 EDT 进行估值，以避免声能衰减曲线上混响时间的拟合范围变化所产生的估值误差^[1]。

测试采用 B&K4138 1/8 英寸无指向性电容传声器，配 B&K2670 前置放大器。声源采用同济大学声学研究所自行开发的小型高频无指向性六面体扬声器，最大线度小于 15mm，实物照片如图 3 所示。声源经 30° 滑动平均在中心频率为 20kHz 倍频带的偏差为 $-1.35\text{dB} \sim +0.93\text{dB}$ ，小于 $\pm 3\text{dB}$ ，符合 ISO3382 对声源指向性所提出的要求。

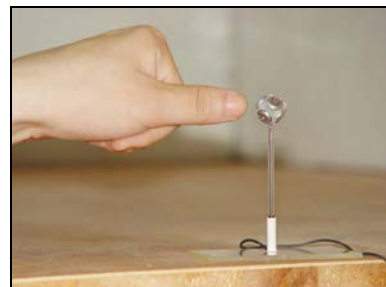


图 3 小型高频无指向性扬声器

3 模型试验结果与分析

3.1 歌剧厅

声源点和接收点的布置如图 4 所示。声源距离舞台地面 7.5cm (相当于实物 1.5m)。接收点共 23 个，高度距离观众席地面 6cm (相当于实物 1.2m)。试验结果如表 1 所示。

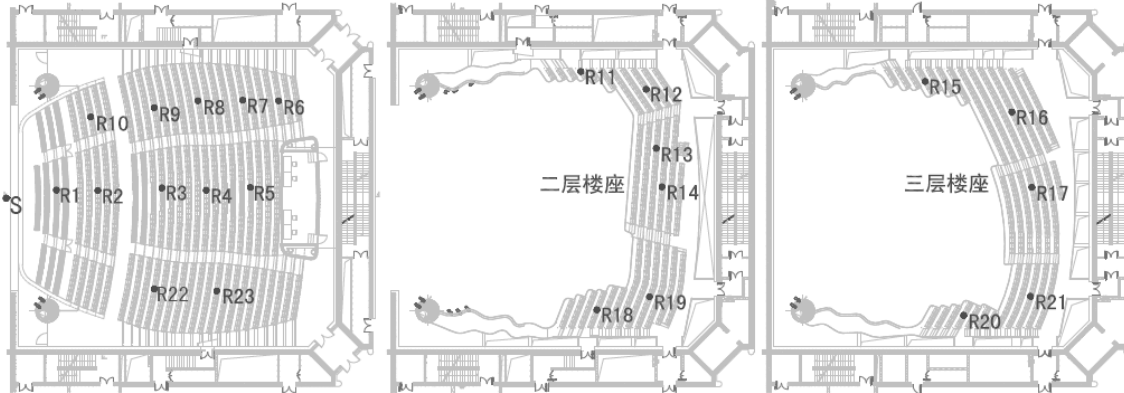


图 4 歌剧厅测点布置图

表 1 歌剧厅测试结果汇总

测点	RT (s)	EDT (s)	G (dB)	D_{50} (%)	C_{80} (dB)
	1kHz	1kHz	1kHz	1kHz	1kHz
池座平均	1.74	1.65	1.64	47.85	1.61
二层楼座平均	1.81	1.61	0.28	50.76	2.31
三层楼座平均	1.85	1.76	0.83	50.23	1.57
全部测点平均	1.78	1.66	1.11	49.12	1.78

缩尺模型 1kHz 混响时间 RT 平均值 1.78s 比设计要求略长。根据我们做模型试验的经验，一般模型测试结果会比实际测试结果略长，考虑到模型和座椅制作材料吸声稍低于实际厅堂中界面的吸声，因此该测试结果符合设计要求。另外，楼座测点的混响时间平均值大于池座测点的混响时间平均值，这与其他大部分歌剧院的实测结果也是吻合的。除个别测点 (R17) 外，各测点的混响时间均与平均值相差较小，表明观众厅中混响时间的分布较为均匀。

缩尺模型 1kHz 早期衰变时间 EDT 平均值为 1.66s，小于其混响时间平均值，衰减曲线呈下凹状，观众厅后期声衰减比早期衰减要慢。声场衰变的这种特性，兼顾了对白时的语言清晰度和音乐时的丰满度的要求。

声场强度 G 平均值为 1.11dB，在设计指标范围内，符合设计要求。观众厅前区测点的 G 值偏大，主要是因为这些测点离声源比较近。此外，在 23 个测点中，最大 G 值与最小 G 值相差 5.52dB，符合 $\leq \pm 3$ dB 的要求，表明观众厅内的声场分布较为均匀。

明晰度 C80 平均值为 1.78，且除个别测点外，C80 值均在设计指标范围 (-1~+3dB) 内。

此外，考察各测点的反射声系列，未出现回声、多重回声、声聚焦和共振等可识别的声缺陷，仅发现 R2 和 R10 两测点在直达声到达后约 35ms 处有一个强反射声。经计算分析认为：该强反射声来自于顶面的反射板。原因是实际设计的顶面反射板呈弧形，而模型实际制作的时候由于制作工艺的关系而用直板替代，由此在观众厅前区某些位置对声线产生强反射，在实际建成厅堂中可以合理预期不会出现上述问题。

3.2 音乐厅

声源点和接收点的布置如图 5 所示。声源距离舞台地面 7.5cm (相当于实物 1.5m)。接收点共 12 个，高度距离观众席地面 6cm (相当于实物 1.2m)。测试结果如表 2 所示。

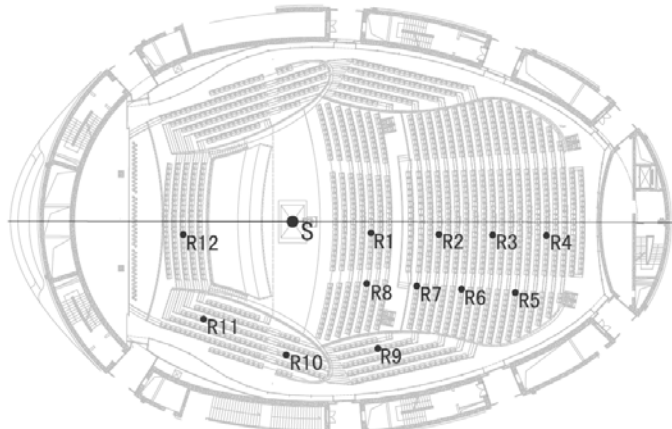


图 5 音乐厅测点布置图

表 2 音乐厅测试结果汇总

测点	$RT(s)$	$EDT(s)$	$G(dB)$	$D_{50}(\%)$	$C_{80}(dB)$
	1kHz	1kHz	1kHz	1kHz	1kHz
全部测点平均	2.49	2.15	6.24	36.44	-0.03

音乐厅模型中频(1kHz)混响时间 RT 平均值为 2.49s, 比设计要求略长。因模型和座椅制作材料吸声稍低于实际厅堂中界面的吸声, 扣除该因素后测试结果应符合设计要求。此外, 除测点 R8 外, 各测点的混响时间与平均值的差值在±0.15 秒范围内, 混响时间的空间分布十分均匀。

1kHz 早期衰变时间 EDT 平均值为 2.15s, 符合 EDT 的设计要求(根据 Beranek 的研究^[2], 对软包座椅音乐厅, EDT 的平均值为 2.2s, 范围从 1.9s 到 2.4s)。EDT 的测试结果进一步印证了前期音质设计对混响时间的控制符合要求。

1kHz 声场强度 G 平均值为 6.24dB, 稍大于设计要求的上限 5.5dB, 原因是模型制作材料的吸声系数略小。观众厅前区测点的 G 值偏大, 主要是因为这些测点离声源比较近, 扣除离声源位置最近的 4 个测点的测试结果后 G 平均值为 5.7dB。此外, 在 12 个测点中最大 G 值与最小 G 值相差仅 2.43dB, 观众厅内的声场分布非常均匀。

1kHz 明晰度 C80 平均值为 -0.03, 符合交响乐对明晰度 -3~0dB 的要求。此外, 考察各测点的反射声系列, 均未发现回声、多重回声、声聚焦和共振等可识别的声缺陷。

4 结论

歌剧厅和音乐厅的音质模型测试结果表明前期声学设计合理, 未发现明显的音质缺陷和声学计算失误。厅内混响时间等主要音质参量的控制符合设计要求, 声场强度满足要求, 声场不均匀度小。两厅均可取得满意的音质效果。

参考文献

- [1] 莫方朔, 盛胜我. 厅堂音质缩尺模型测试中空气声吸收的修正. 中国声学学会 2006 年全国声学学术会议论文集, 2006, 365-366.
- [2] 白瑞纳克 (美) 著, 王季卿等译. 音乐厅和歌剧院[M]. 上海: 同济大学出版社, 2002.

Sound Absorption of Parallel-Arranged MPP Absorbers

WANG Chunqi, HUANG Lixi

(Mechanical Engineering Department, The University of Hong Kong, Pokfulam Road, Hong Kong SAR, PRC)

Abstract: The sound absorption performance of parallel arranged MPP absorbers with different frequency characteristics is addressed. The finite element method is used to simulate the acoustic behavior of the MPP absorber array. Results show that both the bandwidth and absorption level of the MPP absorber array can be increased in comparison with the corresponding single MPP absorbers. The local resonances and near field interaction in the MPP absorber array are examined numerically. Effects of geometrical factors are also considered.

Key words: micro-perforated panel; sound absorption; parallel arrangement

摘要：本文利用有限元方法，对并联微穿孔吸声结构的声学特性进行了仿真计算。研究表明，和单个微穿孔吸声结构相比，并联结构可以得到更宽的吸声带宽、更高的吸声系数；并联结构中的局部共振以及近场相互作用决定了系统的吸声特性。数值研究同时表明，结构的几何因素对吸声特性有明显的影响。

关键词：微穿孔板；吸声结果；并联布置

1 INTRODUCTION

Micro-perforated panel (MPP) absorbers have been used for decades as an attractive alternative to traditional fibrous sound absorption materials [1-5]. A basic MPP absorber consists of an MPP fitted in front of a rigid backing wall, which is usually parallel to the MPP. The resonance-absorption constitutes the fundamental sound absorption mechanism in the MPP absorbers, while the MPP absorbers perform much better than other resonant absorbers, for example, the Helmholtz resonator of larger neck size. However, the sound absorption capability of the MPP absorber is usually still not quite enough as a general-purpose absorber. Both its bandwidth and sound absorption coefficients are insufficient to compete with the fibrous materials.

In order to obtain broadband performance, a straightforward method is to arrange multiple MPP absorbers of different frequency characteristics in parallel to combine different frequency bands together. Previous studies on parallel arrangement of two different MPP absorbers have shown great potential of the parallel arrangement to enhance the sound absorption performance [6-8]. In a recent work, the dominant absorption mechanism in the MPP absorber array was found to be the strong local resonance absorption due to different acoustic reactance matching conditions for the component MPP absorbers [9]. Note that both the MPP properties and the backing cavity depths of the component MPP absorbers can be different to obtain different frequency characteristics. In what follows, the sound absorption performance of parallel arranged MPP absorbers are discussed based on an MPP absorber array with different cavity depths arranged in a periodic pattern. The general observations applies to the MPP absorber array with different perforation properties.

2 THEORETICAL MODEL

Figure 1 shows one module of the MPP absorber array with the backing cavity being partitioned into three sub-cavities with depths D1-D3. The widths of the three cavities, W1-W3, are assumed to be identical, while an arrangement of different cavity widths may provide more flexibility for the absorber design. The cavity walls are assumed to be acoustically rigid. The MPP itself can be either flexible or rigid, depending on the thickness and material of the panel.

Assume a plane wave is incident on the MPP with unit amplitude and an angle of incidence θ ,

$$p_i = e^{i(\omega t - k_0 \cos \theta \cdot x - k_0 \sin \theta \cdot y)} \quad (1)$$

where k_0 is the acoustic wave number, ω is the angular frequency. The sound field in the computation domain ABDC includes the incident sound wave p_i and the scattered sound wave p_{sc} due to the unequal acoustic impedance over MPP absorbers 1-3. The sound filed inside the computational domain ABCD and the backing cavities is modeled by the wave equation,

$$\left(\nabla^2 - \frac{1}{c_0^2} \frac{\partial^2}{\partial t^2} \right) \phi = 0, \quad (2)$$

where ϕ is the velocity potential which is related to sound pressure p and acoustic particle velocity u as,

$$p = -\rho_0 \frac{\partial \phi}{\partial t}, \quad u = \nabla \phi, \quad (3)$$

The acoustic impedance of the MPP is determined by the panel thickness t , orifice diameter d and perforation ratio σ based on Maa's formula^[2].

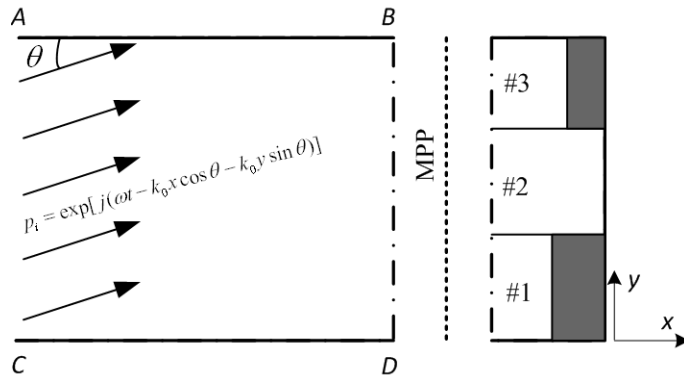


Figure 1: Theoretical model for the MPP absorber array with three different cavity depths arranged in a periodic pattern.

A finite element procedure is established to simulate the acoustic behavior of the MPP absorber array. At the left boundary AC, the incident sound wave p_i is mixed with the unknown scattered sound wave p_{sc} . The Dirichlet-to-Neumann boundary condition^[10] is implemented to allow the scattered sound wave pass through this artificial boundary without reflection. At the bottom and top boundaries, periodic conditions apply. Denote the normal particle velocities (pressure) on the two boundaries by V_d and V_u . (p_d and p_u). The periodic condition can be expressed as,

$$V_d = V_u \cdot e^{ik_0 L \sin \theta} \quad P_d = P_u \cdot e^{ik_0 L \sin \theta} \quad (4)$$

where L is the height of the computational domain.

3 NUMERICAL RESULTS

The acoustic performance of the MPP absorber array under normal incidence ($\theta=0$) is simulated using the finite element method. The geometrical configuration of the MPP absorber array is:

$$D_1=50 \text{ mm}; \quad D_2=100 \text{ mm}; \quad D_3=25 \text{ mm}; \quad W_{1,2,3}=30 \text{ mm}. \quad (5)$$

The parameters of the MPP are chosen as $d=0.5$ mm, $t=0.5$ mm, $\sigma=1$. Figure 2 compares the normal incidence absorption coefficients between the MPP absorber array and the single MPP absorbers. For the MPP absorber array, three spectral peaks are observed at $f=470$ Hz, 650 Hz and 930 Hz with the sound absorption coefficients $\alpha_N > 0.95$. In between the three peaks, the sound absorption is still maintained at a relatively high level, making it possible to design an effective broadband sound absorber based on the parallel combination of multiple MPP absorbers. Another important observation is the enhanced sound absorption performance of the MPP absorber array over the single MPP absorbers. This feature becomes more noticeable when the orifice diameter of the perforated panel becomes large.

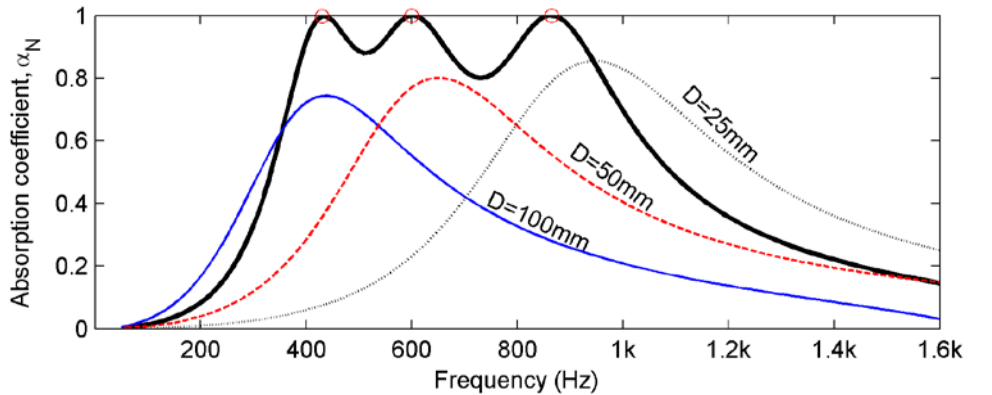


Figure 2: Comparison of the normal incidence absorption coefficients between the MPP absorber array

The acoustic characteristics of the MPP absorber array are determined by the strong local resonances in the system and the near-field interaction effect among different MPP absorbers. These phenomena are examined numerically by visualizing the acoustic field in the neighbourhood of the perforated panel. Figure 3 shows the sound intensity in the duct at $f=470$, 650 and 930 Hz, corresponding to the three spectral peaks in Figure 2. It can be seen that most part of the acoustic energy are “attracted” toward the resonating cavity and dissipated by the MPP covering it.

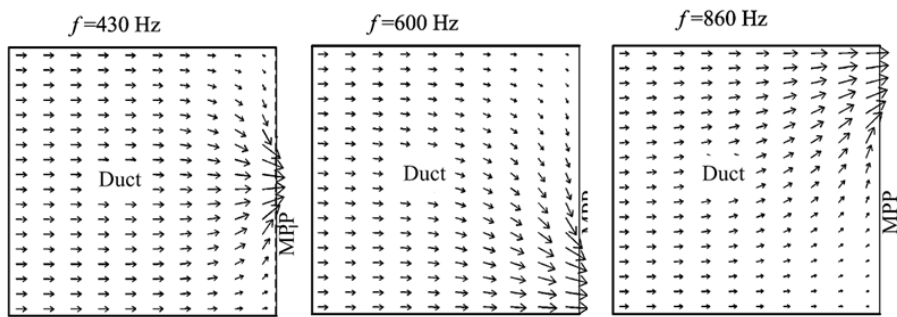
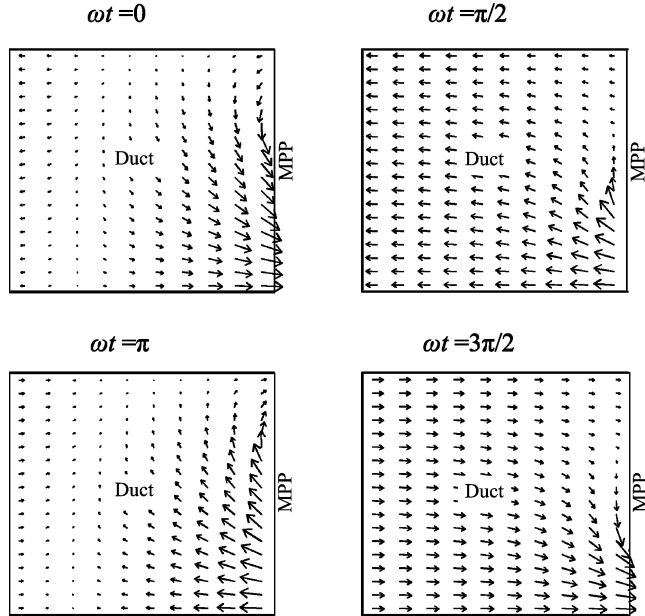
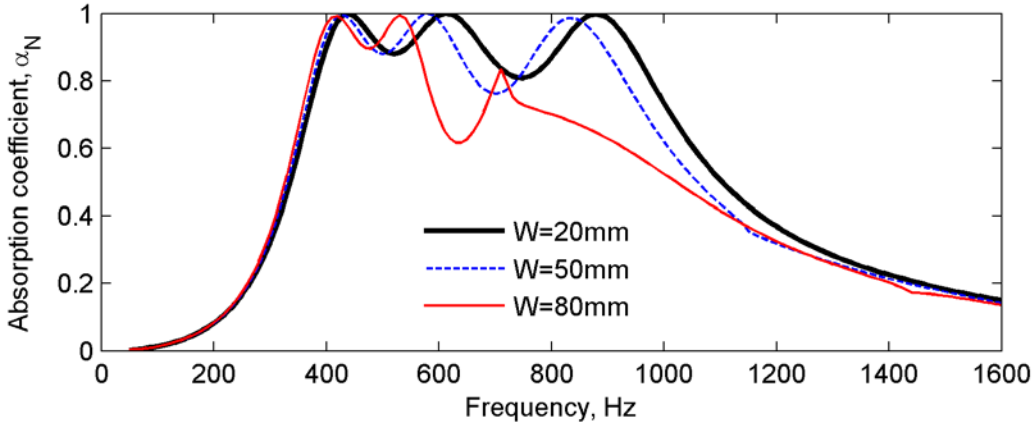


Figure 3: The sound intensity in the duct at the resonance frequencies of the MPP absorber array.

Figure 4 shows the distribution of the instantaneous particle velocity at $f=600$ Hz at the moment $\omega t = 0$, $\pi/2$, π and $3\pi/2$. In the far field of the perforated panel, a flat wavefront is observed as it would be when the perforated panel is backed by a constant air gap. In the near field of the perforated panel, however, the wavefront is distorted greatly because of the non-uniform acoustic impedance across the MPP surface. Obvious acoustic wave propagation between cavity 1 and cavity 3 can be seen. Note that the air motion around cavity 3 is approximately out of phase with that around the resonating region (cavity 1). This phase difference can be attributed to the different distance that the acoustic wave travels within each individual cavity. The near-field cross-talk effect among neighbouring cavities intensifies the air motion through the small micro-perforations where the resonance occurs, and hence enhanced dissipation of the incident acoustic energy is achieved. However, further investigation is required to understand the precise mechanism in more details.

Figure 4: Spatial distribution of the instantaneous particle velocity at $f=600$ Hz in one period.Figure 5: Variation of the normal incidence absorption coefficients with the cavity width. The MPP parameters are: $d=0.8$ mm, $t=0.5$ mm, $\sigma=1$.

The near-field coupling effect decays with the distance between different cavities. So the acoustic properties of the MPP absorber array vary with the sizes and space arrangement of the cavities. Figure 5 shows the variation of the predicted absorption coefficients with the width of the cavity. As the cavity width increases from $W=20$ mm to $W=50$ mm, the second and the third peaks shift to lower frequencies, and the absorption performance decreases between the two peaks. As the cavity width further increases to $W=80$ mm, the absorption level at the first two peaks remains almost unchanged, but the absorption performance around the third peak drops dramatically. In the frequency range from 700 Hz to 1000 Hz, the absorption coefficients of the absorber array is approximately the average of the component MPP absorbers. Note that the centre-to-centre distance between cavity 1 and cavity 3 is $2 \times W=160$ mm, which equals to the quarter wavelength at $f= 540$ Hz. This frequency roughly matches the critical frequency, beyond which the sound absorption caused by the near-field effect cannot sustain.

An equivalent electrical circuit model is established to represent the MPP absorber array when the vibration of the perforated panel is excluded, as shown in Figure 6. The results are shown in Figure 7. For comparison purposes, finite element simulation results with different cavity depth sequences are also given. Sequence 1

corresponds to the arrangement specified in (5). Sequence 2 is chosen as $D_1=50\text{mm}$, $D_2=25\text{mm}$, $D_3=100\text{mm}$. For different cavity sequences, the absorption curves are similar on the whole with almost the same resonance frequencies. The major difference lies in the variations of the sound absorption level at the spectral peaks and in between of them. The effect is nearly negligible when the cavity width is small, but it can be very pronounced when the cavity width is large because the strength of the near-field coupling decays with distance. The equivalent electrical circuit model cannot characterize the influence of these geometrical parameters. In fact, the equivalent electrical circuit model represent the extreme situation in which the characteristic dimension of the MPP absorber array is far less than the acoustic wavelength of interest.

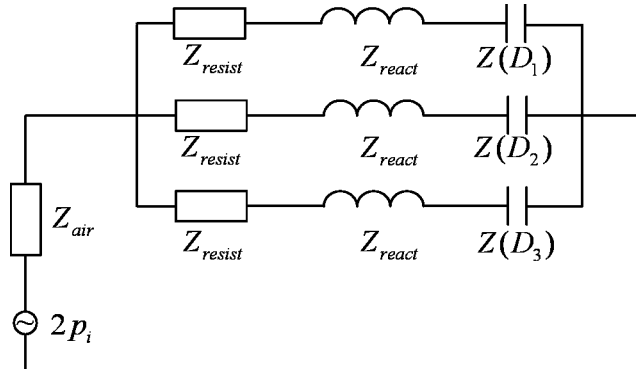


Figure 6: Equivalent electrical circuit analogy of the MPP absorber array

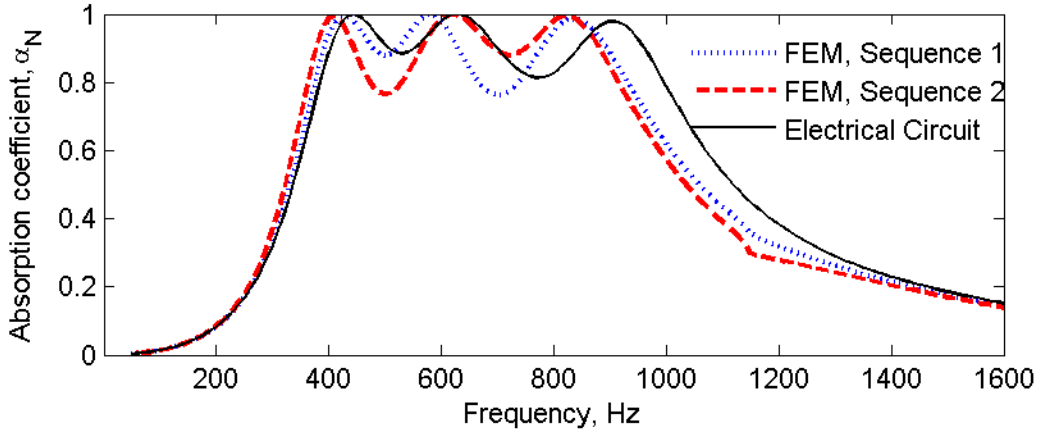


Figure 7: Variation of the absorption coefficients with the arrangement sequences of the cavities in the MPP absorber array.

4 SUMMARY

The sound absorption performance of parallel arranged MPP absorbers with different cavity depths is simulated using a finite element model. Results show that both the bandwidth and absorption level of the MPP absorber array can be increased in comparison with the corresponding single MPP absorbers. The performance improvement of the MPP absorber array is attributed to the strong local resonances and the near field interaction in the system, which are examined numerically. Effects of geometrical factors are also considered. The acoustic properties of the MPP absorber array vary with the sizes and space arrangement of the cavities. The parallel absorption mechanism works when the distance between the component MPP absorbers is less than a quarter-wavelength of the acoustic wave.

ACKNOWLEDGEMENTS

The work was supported by a grant (ITS/095/10) from the Innovation and Technology Commission of the Hong Kong Special Administration Region, China.

References

- [1] Maa DY. Theory and design of micro perforated-panel sound absorbing construction [J]. *Scientia Sinica*, 1975, **18**: 55–71.
- [2] Maa DY. Microporforated Panel wide-band absorber. *Noise Control Engineering Journal* [J], 1987, **29**: 77-84.
- [3] Kang J, Brocklesby MW. Feasibility of applying micro-perforated absorbers in acoustic window systems [J], *Applied Acoustics*, 2005, **66**: 669-689.
- [4] Fuchs HV, Zha X. Micro-perforated structures as sound absorbers- A review and outlook [J]. *Acta Acustica United with Acustica*, 2006, **92**: 139-146.
- [5] Allam S, Åbom M. A new type of muffler based on microporforated tubes [J], *ASME Journal of Vibration and Acoustics*, 2011, **133**: 031005
- [6] Zha X, Kang J, Zhang T, Zhou X and Fuchs HV. Application approach for microporforated panel sound absorbers [J], *Acta Acustica*, 1994, **19**: 258-265.
- [7] Yairi M, Takebayashi K, Sakagami K and Morimoto M. Wideband sound absorber obtained by combination of two micro-perforated panel absorbers with different air cavity depths arranged in parallel [C], *Proceedings of inter-noise 2009*, Ottawa, Canada, August 23-26, paper no. 341
- [8] Wang P, Wang MQ, Liu YS, Zhang JF and Luan HX. Study on the parallel microporforated panels [J], *Piezoelectrics & Acoustooptics*, 2008, **30**: 489-491
- [9] Wang CQ and Huang LX. On the acoustic properties of parallel arrangement of multiple micro-perforated panel absorbers with different cavity depths [J], *Journal of the Acoustical Society of America*, 2011, **130**: 208-218.
- [10] Keller JB and Givoli D. Exact non-reflecting boundary conditions [J], *J. Comput. Phys.* 1989, **82**: 172-192.

语音私密性的掩蔽实验研究

Experimental Study on Achieving Speech Privacy using masking noise

张晓洁¹, 岑文娟², 毛东兴¹

ZHANG Xiao-jie, CEN Wen-juan, MAO Dong-xing

(1. 中华人民共和国 上海同济大学 声学研究所 2. 上海圣戈班石膏建材(上海)有限公司)

(1.Institute of Acoustics, Tongji University, Shanghai 200092,China

2. Saint-Gobain Gypsum (Shanghai) Co., Ltd, Shanghai 201201,China)

Abstract: Speech privacy is an important index for the acoustic performance of public spaces, and it was usually improved by introducing masking noise. Speech intelligibility tests were carried out by using recorded male and female Mandarin words and sentences as speech signals, and air-conditioner and babble noise as masking noise. The masking performance of two noise signals to male and female speech under different signal to noise ratio (SNR) was analyzed, and relationship between speech intelligibility (SI) and signal to noise ratio (SNR) was derived. Results showed babble noise a 7~10dB higher performance in words masking, and 5~7dB higher performance in sentence masking, in comparison with masking performance of air-conditioner noise.

Key words: masking; speech privacy; speech intelligibility; signal to noise ratio

摘要：语言私密性是公共空间中重要的声学问题，利用声掩蔽的方法是改善语音私密性的必要措施之一。采用录制的普通话词语和句子，对处于空调和babble噪声掩蔽下语音信号的语言可懂度进行测试，分析两种掩蔽声在不同信噪比条件下对语音信号掩蔽能力及其差异，获得空调噪声和babble噪声对语音信号掩蔽时语言可懂度(SI)随信噪比(SNR)的变化趋势特征。结果表明，与空调噪声相比，babble噪声对语音的掩蔽能力更强，对词语的掩蔽能力高约7~10dB，对句子的掩蔽能力高约5~7dB。

关键词：声掩蔽；语音私密性；可懂度；信噪比

近年来，在开放型办公室、医院候诊室等公共空间中，语音私密性^[1]越来越引起人们的关注，而利用声掩蔽方法是改善语音私密度的主要途径。T. Tamesue^[2]通过无意义稳定噪声对语言私密度影响实验探讨了articulation index (AI) 和spectral distance (SPD) 哪个更适合对语言私密度的评价，并且实验结果与预计比较，结果表明在语言私密度等级评价中SPD比AI更有效。Komiyama^[3]对混杂各种语音但不包含被掩蔽信号的babble掩蔽声(SI)，以及包含被掩蔽信号的babble掩蔽声(SD)对语言可懂度影响，发现在SD掩蔽声下的语言可懂度比在SI掩蔽声下低 20%~40%。本文通过主观实验研究空调噪声和babble噪声在不同信噪比情况下对语言可懂度的影响，分析了两种掩蔽噪声对语音信号的掩蔽能力及其差异，并对懂度(SI)随信噪比(SNR)的变化的函数模型^[4]进行了改进。

1. 实验设计

1.1 实验信号

实验语料为从汉语普通话语句测听句表中选择的4组实验词语(每组10个单词)，以及11个句子。在听音室录制男声及女声各一组作为实验语声信号，录制时语音的声压级控制在60dB左右。对录好的语声信号再采用Artemis 3.0进行调整使其声压级准确为60dB。调整空调和babble噪声信号分别生成声压级为60dB、64dB、68dB、72dB、76dB、80dB的掩蔽噪声信号，最后用Adobe Audition

合成信噪比为 0、-4、-8、-12、-16、-20dB 的空调噪声和 babble 噪声下的实验信号。

1.2 实验过程

实验在听音室中进行。采用三级评分法：1 分表示完全听不见语音信号；2 分表示听见语音信号但没有听懂其内容；3 分代表完全听懂语音信号。

实验信号通过 SQLab II 系统，采用 HPS IV 均衡器和 Sennheiser HD600 耳机进行回放。受试者共 40 名(22 女/18 男)，年龄在 18 到 23 岁之间，均为在校大学生，自述没有听力障碍。

2. 实验结果分析

2.1 数据处理

对词语语音信号数据，计算每一组的几何平均值，并对其求相关系数，剔除相关系数 10% 左右偏离平均值较远者，重新计算几何平均值。对句子语音信号采用相同的处理方法，把所得分值转化为识别率也即语音信号的可懂度百分值。最终得到空调噪声和 babble 噪声条件下语音信号测试的可懂度百分值。

2.2 词语的掩蔽效果

图 1 中给出了空调噪声及 babble 噪声下男女声词语测试的可懂度(SI)与掩蔽声信噪比(SNR)的关系。

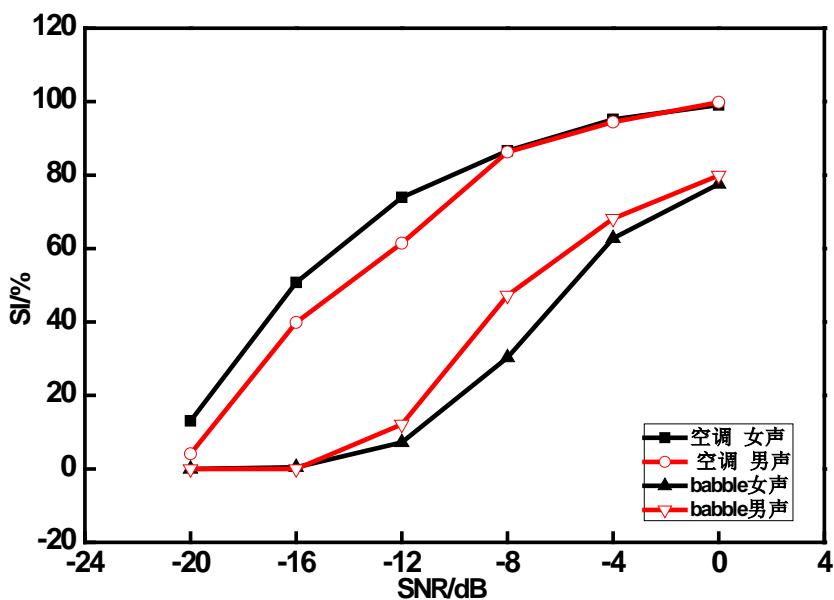


图 1 空调噪声和 babble 噪声隐蔽下词语可懂度对比

图 1 的结果表明，在两种掩蔽声条件下，语音可懂度随信噪比的降低呈非线性下降趋势，但 babble 噪声的下降趋势更快。从图中可以看出 babble 噪声的掩蔽能力明显高于空调噪声的掩蔽能力：在信噪比为 0dB 时，babble 噪声的语言可懂度比空调噪声低约 20%，随着信噪比的下降，两者差异也增大，到信噪比为-12dB 时，两者的 SI 差异达到 60%。

在男女声信号掩蔽效果差异方面，空调噪声在 $SNR < -8dB$ 时对男声的掩蔽能力更强。与此相反，babble 噪声对女声的掩蔽能力高于对男声的掩蔽能力，信噪比为-8dB 时，男声的语言可懂度比女声高出近 20%。从噪声的频谱特性来解释：男声的语音频谱侧重于低频，一般空调噪声具有明显的低频成分，所以有利于男声的掩蔽，而女声的语音频谱侧重于中高频，而 babble 噪声中高频非常明显，所以对于女声语音更有利掩蔽。

2.3 句子的掩蔽效果

图 2 给出了两种掩蔽声条件下，男女声句子测试的可懂度与信噪比的关系。